Original article

Neuroprotective efficacy of 4-Hydroxyisoleucine in experimentally induced intracerebral hemorrhage

Ehraz Mehmood Siddiqui [a,1], Sidharth Mehan [a,1], Shubham Upadhayay [a], Andleeb Khan [b,*], Maryam Halawi [c], Azhar Ahmed Halawi [d], Rana M. Alsaffar [e]

[a] Neuropharmacology Division, Department of Pharmacology, ISF College of Pharmacy, Moga, Punjab, India
[b] Department of Pharmacology and Toxicology, College of Pharmacy, Jazan University, Jazan 45142, Saudi Arabia
[c] Department of Clinical Pharmacy, College of Pharmacy, Jazan University, Jazan, Saudi Arabia;
[d] College of Medicine, Jazan University, Jazan, Saudi Arabia
[e] Department of Pharmacology & Toxicology, College of Pharmacy Girls Section, Prince Sattam Bin Abdulaziz University, P.O.Box-173, Al-Kharj 11942, Saudi Arabia

ABSTRACT

Intracerebral hemorrhage (ICH) is a severe form of brain injury, which is a major cause of mortality in humans. Hydrocephalus and cerebral hematoma lead to severe neurological deficits. A single autologous blood (ALB) injection in rats' brains induces hemorrhage and other conditions that regularly interfere with the standard treatment of several cellular and molecular pathways. Several studies have found that IGF-1/GLP-1 decreases the production of inflammatory markers in peripheral tissues, while some have found that they also have pro-inflammatory functions. Since these receptors are down-regulated in hemorrhagic situations, we looked into the potential neuroprotective effect of 4-hydroxyisoleucine (4-HI); 50 mg/kg and 100 mg/kg, an active compound Trigonellafoenum-graecum, on post-hemorrhagic deficits in rats. Long-term oral administration of 4-HI for 35 days has improved behavioral and neurochemical deficits and severe pathological changes and improved cellular and molecular markers, apoptotic markers in the ALB-induced ICH experimental model.

Furthermore, the findings revealed that 4-HI also improved the levels of other neurotransmitters (Ach, DOPA, GABA, glutamate); inflammatory cytokines (TNF-alpha, IL-1β, IL-17), and oxidative stress markers (MDA, nitrite, LDH, AchE, SOD, CAT, GPx, GSH) in the brain when evaluated after Day 35. There is no proven treatment available for the prevention of post-brain hemorrhage and neurochemical malfunction; available therapy is only for symptomatic relief of the patient. Thus, 4-HI could be a potential clinical approach for treating post-brain haemorrhage and neurochemical changes caused by neurological damage. Furthermore, 4-HI may be linked to other standard therapeutic therapies utilized in ICH as a potential pharmacological intervention.

© 2021 The Author(s). Published by Elsevier B.V. on behalf of King Saud University. This is an open access article under the CC BY-NC-ND license (http://creativecommons.org/licenses/by-nc-nd/4.0/).

1. Introduction

ICH is a worsening scenario worldwide for all stroke conditions (Powers, 2010). ICH is the worse type of subarachnoid and intraventricular hemorrhages that can lead to paralysis, hydrocephalus, and death (Nieuwkamp et al., 2000). It is caused by the destruction of small blood arteries caused by severe hypertension or amyloid angiopathy, which occurs in 80 to 90% of cases (Rajdev et al., 2020; Rajdev and Mehan, 2019). Secondary ICH accounts for fewer cases than primary ICH, which causes due to vascular abnormalities, trauma, tumors, or defective coagulation (Porcari et al., 2018; Aronowski and Hall, 2005; Xue and Del Bigio, 2003). ICH's final consequences result in primary damage due to the expansion of hematoma, thereby applying mass effect and shear force on the cerebral tissues (Ren et al., 2018; Wang and Tsirka, 2005). It can also lead to brain swelling and continuous rupturing of the blood–brain barrier (BBB) (Nadeau et al., 2019; Power et al., 2003). There is no effective therapy or FDA-approved drug to improve the physical and mental condition of brain haemorrhage patients

(Uozumi et al., 2014; D'Ambrosio et al., 2005). ICH's pharmacological intervention and pathophysiologies have been studied using a variety of experimental models, including autologous blood injection, micro balloon model, bacterial collagenase injection model, and double injection model (Alharbi et al., 2016; Deinsberger et al., 1996; Sansing et al., 2011). As a result, we used the rat autologous blood injection model in our research because it closely mimics ICH pathophysiology. The absolute mechanism of ICH, on the other hand, has yet to be fully proved. Increased intracranial pressure and acute vasoconstriction are the two critical factors responsible for lowering cerebral blood flow in ischemic conditions (Rajdev et al., 2020; Tschoe et al., 2020; Kirkman et al., 2011).

However, Insulin-like growth factor 1(IGF-1)/Glucagon-like peptide-1(GLP-1) has an essential role in the neuroinflammatory response (Labandeira-Garcia et al., 2017). The expression of inflammatory markers has been obstructed in peripheral tissues (Lee and Jun 2016). Other studies reveal that both of them had pro-inflammatory functions in which TNF-α damaged the signaling of IGF-1/GLP-1 (Tien et al., 2017; Carro et al., 2003).

The choroid plexus carries IGF-1 thoroughly to the central nervous system (CNS) (Suh et al., 2013). Also, it is indigenous to the brain and has a neuroprotective effect (Serhan et al., 2020). IGF-1 has several CNS effects (Santi et al., 2018), early brain development regulation, myelination, synapse development (Nieto-Estévez et al., 2016), neurogenesis, neurotransmitter production, and cognition (Wrigley et al., 2017). A previous study reported that the upregulation of GLP-1 shows neuroprotection in the brain injury in rat brain after subarachnoid hemorrhage (Park et al., 2011; Tien et al., 2017). Psychological distress and other neurodegenerative brain disorders have also been reported to have decreased IGF-1, indicating the use of IGF-1 as a possible treatment (Shandilya and Mehan, 2021; Rodriguez-Perez et al., 2016). In the presence of glia, IGF-1 protecting neurons against neurotoxins related to glia directly mediated by IGF-1(Rodriguez-Perez et al., 2016; Nadjar et al., 2009).

GLP-1R is found in the brainstem nucleus, substantia nigra, cerebellum, circumventricular system, hypothalamus, amygdala, hippocampus, and cerebral cortex (Athauda and Foltynie, 2016; Heppner et al., 2015a, 2015b). Several brain functions are regulated by GLP-1 and its agonists, such as neurogenesis (Grieco et al., 2019), retinal repair (Katsurada and Yada, 2016), thermogenesis, blood pressure (Rowlands et al., 2018), neurodegeneration (Wang et al., 2020), and energy homeostasis alteration (Baggio and Drucker, 2014). GLP-1 pre-glucagon neurons arise from the brainstem solitary tract (Llewellyn-Smith et al., 2011) and are approached to the cortical regions, thalamus, hypothalamus, and thus, inducing the transit of GLP-1 (Geloneze et al., 2107; Katsurada and Yada, 2016). GLP-1 analogues can cross the BBB and have several effects on endogenous GLP-1(Athauda and Foltynie, 2016), such as anorexigenic and neuroprotective effects (Cabou and Burcelin, 2011) in various neurodegenerative diseases. GLP-1 treatment has been shown to be effective in a variety of other neurodegenerative disorders, such as Alzheimer's disease (Gengler et al. 2012), Parkinson's disease (Bertilsson et al. 2008), Amyotrophic lateral sclerosis (Shandilya and Mehan, 2021), Peripheral neuropathy (Himeno et al. 2011). Multiple sclerosis-related animal model studies (Rossi et al. 2012; Holt and Trapp, 2016; Shiraishi et al., 2012).

In the current investigation, neuronal stability and neurodegeneration prevention were restored with 4-hydroxyisoleucine (4-HI). *Trigonellafoenum L.* Fenugreek (Fabaceae) has a solid tradition of Ayurvedic and Chinese medicine. 4-HI is an insulinotropic, biochemical, natural non-protein acid amino acid. It is a principal active constituent of *Trigonellafoenum graecum* L, representing around eighty percent of the overall free amino acid content (Avalos-Soriano et al., 2016). 4-HI is structurally identical to a branched amino acid having an insulinotropic effect and directly improves insulin sensitivity (Gao et al., 2015; Broca et al., 2004). It also has been reported to act as a neuroprotective agent in various conditions such as hypocholesterolemic, anti-oxidant, hepatoprotective (Kumar et al., 2012), reduce brain inflammation (Moghadam et al., 2013), and anti-carcinogenic (Rampogu et al., 2018).

Treatment with 4-HI restored cellular anti-oxidant enzymes' altered function in tissues such as the brain, muscle, and heart (Baquer et al., 2011). It was found that 4-HI binds to GLP-1 and increases the ability of GLP-1 to activate GLP-1R signaling, and plays a significant role in improving glucose excursions in diabetes mellitus (Xue et al., 2011). 4-HI stimulates proximal insulin signaling, increases glycogenic enzymes and Glucose transporter 2 (GLUT2) expression in HepG2 cells (Mohammed and Islam, 2018). 4-HI alleviates lipopolysaccharide (LPS)-induced inflammation via the iRhom2-dependent pathway in co-cultured macrophages and adipocytes(Zhou et al., 2020). The activation of the insulin/GH/IGF-1 axis, which causes increased mammalian sensitivity to these hormones, is likely to result in 4-HI in milk production (Sevrin et al., 2020). Clinical reports showed that ingestion of 4-HI (1 mmol/kg lean body mass) decreased blood glucose levels and increased gluconeogenesis after four hours post-administration time in normal subjects (Nuttal et al., 2006). Furthermore, IGF-1/GLP-1 may protect the developing brain from chronic inflammation (Harkavyi and Whitton, 2010; Pang et al., 2010). IGF-1/GLP-1 is currently being studied to treat the nervous system's pathologies due to its effective longevity and differentiating function. As a result, the primary goal of this study was to look into the neuroprotective effects of 4-HI on behavioural, molecular, neurochemical, and gross pathological changes in ALB-induced ICH rats, specifically to confirm the dysregulation of IGF-1 and GLP-1 signaling pathways in ICH progression.

2. Materials and methods

2.1. Experimental animals

Thirty-six male Wistar rats weighing between 180 and 220 g were used in the study. Rats were procured from the Central Animal House, ISF College of Pharmacy, Moga, Punjab, India (Ethical clearance number: 817/PO /ReBiBt/S/04/CPCSEA). Free access for all laboratory animals to food and water. Animals were allowed to acclimatize for at least one week before the start of the experiment. Behavior parameters were examined between 9 a.m. to 5p.m.

2.2. Chemicals used

The 4-hydroxyisoleucine (4-HI) protocol drug was acquired as ex-gratia samples from BAPEX Pharmaceuticals, India. Ketamine (75 mg/ml; Paksons Pharma Pvt. Ltd.), Heparin sodium injection (25,000 IU units per 5 mL; Biological E limited), glucose powder (99.4%, Glucon D), pads for sterile alcohol preparation (Dynarex Corporation), Sterile solution of saline (0.9 % (wt/vol) NaCl in distilled water). Ketoprofen (100 mg; Actiza pharmaceuticals private limited), Neomycin (10 g; Intas biopharmaceuticals), Gentamycin (80 mg; Dheer healthcare private limited), Lignocaine gel (Lox 2% Jelly; Cadila pharmaceuticals), Sodium pentobarbital (270 mg/ml, i.p; SBS biotech). 4-HI was dissolved in an aqueous solution with 2% ethanol and was orally administered (p.o.) (Gaur et al., 2012). All other chemicals used in the study are of analytical grade. Drug and chemical solutions were freshly prepared before use.

2.3. Protocol schedule of animal experimentation

The overall research period was of 35 days. The intracerebroventricular (ICV) blood autologous (ALB) was administered with a Hamilton syringe on day zero. 4-HI was systematically administered from 1st day to the 35th day of the research protocol. In the study, none of the standard drugs was used. All the animals were randomly assigned to six groups with six animals each. Group 01: Vehicle control, Group 02: sham control, Group 03: 4-HI perse (100 mg/kg, p.o.), Group 04: ALB (20 µl, i.c.v.), Group 05: ALB (20 µl, i.c.v.) + 4-HI (50 mg/kg, p.o.), Group 06: ALB (20 µl, i.c.v.) + 4-HI (100 mg/kg, p.o). As shown in Fig. 1, behavioral parameters were accessed from the first day to day 35. There was a 14-days difference in each group to overcome the overlapping of experimental groups on behavioral instruments and smooth conduction of all analysis. Animals were anesthetized with pentobarbital sodium, and the brain was removed carefully. All biochemical parameters were performed in the whole-brain homogenate.

2.4. Developement of ICH model

The rats were anesthetized by ketamine (75 mg/kg, i.p.), and through stereotaxic apparatus, the ALB-induced experimental model of ICH was established by Rajdev et al., 2020 (Rajdev et al., 2020). Animals are then supplemented by a standard diet of water and chow. The body weight was assessed on days 1, 7, 14, 21, 28, and 35 of the experiment.

2.5. Parameters assessed

2.5.1. Behavioral parameters
2.5.1.1. Morris water maze (MWM) task. MWM was used to test the cognitive functions by evaluating the escape latency on days 32, 33, 34 and the time spent in the target quadrant (TSTQ) measured on day 35. As described by Duggal et al., 2020, the protocol was designed and performed (Duggal et al., 2020). Before surgery, training was given to animals, and then they were randomly divided into different groups. The working memory was executed 30 s after hemorrhage induction on the day, and escape latency was also measured. On day 35, rats were tested, and a TSTQ assessment was carried out, and the platform was removed.

2.5.1.2. Forced swim test (FST). Following the ICH procedure and minor modifications, each rat undergoes FST on days 7, 14, 24, and 34 (Roh et al., 2016, Boyko et al., 2013). Rats were individually placed in cylinder tanks (with 30 cm water at 24 ± 1 °C; height: 50 cm; diameter: 15 cm). The movement of the rat was equipped with a camera for five minutes. All observational rats were subjected to a 15-minute pre-test to remove the water's acute stress and ensure the capacity to adapt to water for animals. The animals were tested for 5 min, twenty-four hours after the pretest. The immobility time was measured to subtract the total time of mobility over the test's 5 min. If the rat stopped moving and was still floating in a smooth place in the water, it was justified that the rat was stable, making small moves to keep his head above the water.

2.5.1.3. Beam crossing task (BCT). After surgery, beam-walking (1.0 cm in diameter, beam long 80 cm) was performed to quantify neurological scores in the hind limbs during days 1, 15, 25, and 35. The scoring was performed according to (Sharma et al., 2019).

2.5.1.4. Locomotor activity. The locomotor activity was monitored by actophotometer (INCO, Haryana) on days 7, 14, 21, 28, and 35. Briefly, the animals were habituated by placing them individually for 3 min in the activity room. After that, over five minutes, each animal was seen and shown as a count for five minutes (Mehan et al., 2018).

2.5.1.5. Novel object recognition test. A protocol of Cohen et al., 2015 has been used to test every rat on days 1, 15, 25, and 35 after the ICH for the novel object recognition test. The discrimination index (DI) was calculated as follows:

$$\{(novel object - familiar object)/(familiar object + novel object)\} \times 100$$

2.5.2. Biochemical parameters
2.5.2.1. Brain homogenate preparation. The homogenate of the brain was prepared by the method of Javanshir and Hemmati, 2020. The sample was stored at $-80\ ^{\circ}C$ for use in the future. The whole-brain homogenate was used for the assessment of all parameters.

2.5.2.2. Measurement of IGF-1/GLP-1 and MBP levels. To quantify the IGF-1/GLP-1 (Candeias et al., 2018; Ola et al., 2014) and myelin basic protein (MBP) (Khan et al., 2006) levels in rat brain homogenates, a diagnostic kit (E-EL-R0010/ IGF-1; E-EL-R3007/GLP-1; E-EL-R0642/MBP; Elabsciences, Wuhan, Hubei, China) was used in the experimental protocol. As outlined in the kit, samples and all reagents were prepared with minor alterations according to the manufacturers' protocol. A Bio-Rad iMark 96-well plate reader was used to measure the absorbance at 450 nm. The results have been shown as nanogram per milligram protein.

2.5.2.3. Measurement of apoptotic markers (Caspase-3 and Bax, Bcl-2) levels. For the measurement of Caspase-3 (Wang et al., 2002) and Bax (Tiwari et al., 2021), Bcl-2 (Bai et al., 2019; Moneim, 2015) levels in rat brain homogenates, a diagnostic kit (E-EL-R0160/ Caspase-3; E-EL-R0098/Bax/Bcl2Elabsciences, Wuhan, Hubei, China) was used. As outlined in the kit, all reagents and samples were prepared with minor alterations according to the manufacturers' protocol. A Bio-Rad iMark 96-well plate reader was used for 450 nm absorbance measurement. The results have been shown as nanogram per milligram protein.

2.5.3. Neurotransmitter's evaluation
2.5.3.1. Glutamate and Gamma-Aminobutyric acid (GABA) levels. The GABA and glutamate levels were evaluated using the Donzanti (Rajdev et al., 2020, Donzanti and Yamamoto, 1988) process, with minor modifications to the High-performance liquid chromatography (HPLC) and Electrochemical detector (ECD) system. A standard procedure for Waters consisting of an isocratic high-pressure pump, a manual sample was used. Twenty microliter injector valve, C18 reverse phase. In the study, ECD was used. Use Breeze Software Version 3.2 to process and cataloged data. The amino acid levels within the 10–100 ng/ml concentration range are calculated using a standard curve. Data presented as an ordinary control group proportion.

2.5.3.2. Acetylcholine (Ach) levels. Ach levels were measured by (E-EL-0081/acetylcholine; ELabSciences, Wuhan, Hubei, China) Elisa kit. All reagents and samples were prepared according to the instructions specified. The absorbance was recorded at 540 nm (Zeng et al., 2017).

2.5.3.3. Dopamine (DOPA) levels. Brain dopamine levels were estimated by the method described by Broca et al., 2004 (Broca et al., 2004). Data collection and analysis were carried out using Breeze software. Electrochemical detector sensitivity (ECD) ranged from 5 to 50 nA.
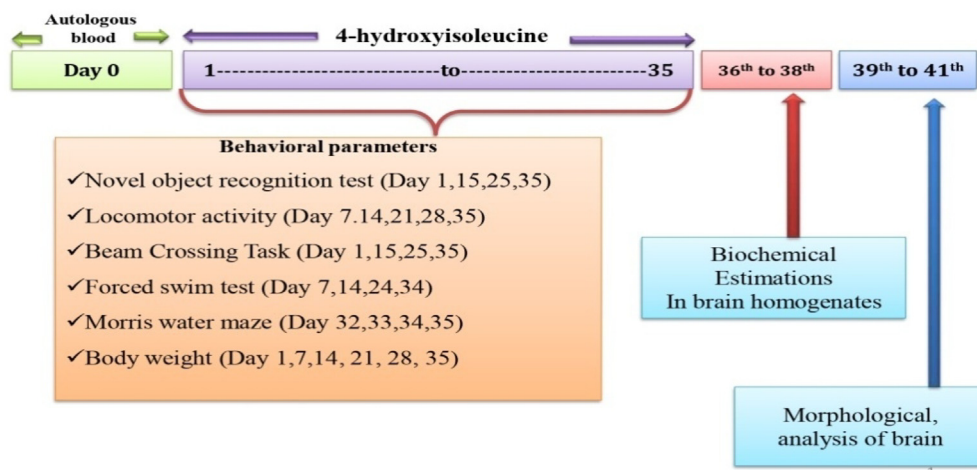
Fig. 1. Experimental protocol schedule of the study.

2.5.4. Evaluation of neuroinflammatory cytokines
2.5.4.1. TNF-α, IL-1β, and IL-17 levels. The ELISA kits were used to analyze the inflammatory cytokines such as TNF-α, IL-1β, and IL-17 (E-EL-R0019/TNF-α; E-EL-R0012/IL-1β; E-EL-R0566/IL-17; ELabSciences, Wuhan, Hubei, China). Absorbance was determined at 450 nm on the microtiter plate (Sharma et al., 2021; Wang et al., 2018).

2.5.5. Evaluation of oxidative stress markers
2.5.5.1. Acetylcholinesterase (AChE) levels. AChE activity is determined by Ellman's method, as described (Rajdev et al., 2020; Ellman et al., 1961). The mixture of the test's composition consisted of 0.05 mL of supernatant, 3 mL of 0.01 M of sodium phosphate (pH 8), 0.10 mL of acetylthiocholine iodide, and 0.10 mL of DTNB. In μmol/mg protein, the enzymatic activity was indicated.

2.5.5.2. Superoxide dismutase (SOD) levels. The activity of the total SOD was assessed by Dudi (Dudi and Mehan, 2018). SOD activity was expressed as units/mg of protein.

2.5.5.3. Reduced glutathione (GSH) levels. The Ellman method estimates brain glutathione levels (Ellman, 1959). The glutathione levels are expressed in the supernatant as μM/mg protein (Alam et al., 2020).

2.5.5.4. Lactate dehydrogenase (LDH) levels. For the estimation of the total LDH, the UV-spectrophotometric method was used. LDH activity was measured using an LDH kit (Transasia Bio-Medicals Ltd., Mumbai, India) in the rat brain homogenate, and it was expressed as IU/L (Mehan et al., 2020)

2.5.5.5. Glutathione peroxidase (GPx) levels. GPx ELISA kit (E-EL-R2491/GPx; ELab science, Wuhan, Hubei, China.) was used for the evaluation, and the method was used as in the instructions. The absorption rate decreased to 340 nm per minute by taking the average rate of changes between 30 and 180 s for 30 s (Wang et al., 2018).

2.5.5.6. Malondialdehyde (MDA) levels. Quantitative measurements were taken using the Wills method for the lipid peroxidation in the brain homogenates as end product MDA. The MDA protein concentration was indicated as nM/mg protein (Rahi et al., 2021).

2.5.5.7. Nitrite (NO) levels. Greiss reagent test was used to estimate NO levels as described by Abdel-Rehman et al., 2020. (Abdel Rehman et al., 2020).

2.5.5.8. Catalase (CAT) levels. The catalase activity was determined by measuring the decomposition of H_2O_2 using at 240 nm spectrophotometer described by Aebi's method in serum and brain homogenates (Aebi, 1984). The CAT activity was estimated and expressed in the U/g brain protein.

2.5.6. Total protein levels
The protein content was measured with the Coral Protein Estimate Kit using the biuret method (Minj et al., 2021).

2.5.7. Assessment of gross pathology and hematoma size in rat brain
After the experiment, on the 36th day, brains were removed by decapitation. The brains of animals were examined, and coronal sections were further used to study the morphological alterations (Rajdev et al., 2020; Liu et al., 2015). The brain was quickly removed for hematoma size measurement and further submerged in ice-cold saline for 1 min. To determine hematoma volume, a tissue was then placed on the chopper. The 2 mm thick brain section has been placed on the glass. A digital camera (Sony A7 III digital camera, Japan) was used to perceive all brain areas that encompass the entire striatum. The digital images of all brain areas, including hematoma, took less than five minutes on each part of the brain. The captured digital images have been filtered for illustration purposes. They were converted into TIFFs. After completing the procedure, the hematoma region (mm) in each brain section was measured using the image MOTICAM-BA310 plus 2.0 analysis software (after Day 36).

For each segment of the coronal brain, the volume of the hematoma scale (mm^3) was measured by the hematoma region (mm) (Terai et al., 2003). On day 36, after ICH was induced from the striatum's red surface, the hematoma dimensions (mm^3) were measured in each brain segment. The hematoma size was calculated with the formula ($l \times b \times h$) by calculating the hematoma's surface area in every 2 mm thick coronary brain section (Kumar et al., 2021).

2.6. Statistical analysis

Data were analyzed using two-way ANOVA followed by Post hoc test Bonferroni and one-way ANOVA repeated measures followed by Post hoc test Tukey's multi comparison test. $P < 0.001$

was considered statistically significant. Data was found to be normalized, and the sample size was calculated by checking the normality distribution by the Kolmogorov Smirnov test. All statistical results were performed out by GraphPad Prism version 5.03 for Windows (GraphPad Software, San Diego, CA, USA). Statistical results were expressed as the mean ± standard error of mean (SEM).

3. Results

3.1. Effect of 4-HI on body weight in rats treated with ICH

We have been monitoring body weight according to the protocol duration of 1, 7, 14, 21, and 28 days to explore the therapeutic potential of 4-HI in ALB-induced ICH. On day 01, all groups did not differ significantly. In contrast to vehicle and sham rats, rats' body weight decreased substantially to cause hemorrhage with ALB. 4-HI 100 mg/kg treatment perse did not show any body weight change over vehicle rats. Consistent 4-HI 50 mg/kg therapy and 4-HI 100 mg/kg successfully reversed ALB weight loss in comparison to vehicles and 4-HI 100 mg/kg premedication [Two-way ANOVA: $F_{(25,150)} = 50.67$, $p < 0.01$] (Fig. 2).

3.2. Behavioral parameters

3.2.1. Effect of 4-HI on escape latency and the TSTQ in rats treated with ICH

During the MWM test, the escape latency in the training rats gradually decreased. The escape time of the ALB group induced ICH in rats increased on days 32, 33, 34, 35 in comparison to the vehicle group [Two-way ANOVA: $F_{(10,60)} = 30,74$, $p < 0.01$]. Treatment of 4-HI 100 mg/kg perse showed no difference in escape latency than vehicle control rats. Chronic 4-HI 50 mg/kg and 4-HI 100 mg/kg latency treatment decreases the following hemorrhage. On day 35, TSTQ was reduced to 4-HI 100 mg/kg in hemorrhagic mediated rats of ALB compare to vehicle control rats. The TSTQ improved significantly in chronic 4-HI 50 mg/kg and 4-HI 100 mg/kg groups [Two-way ANOVA: $F_{(5,25)} = 3,859$, $p < 0.01$] (Fig. 3; Fig. 4).

3.2.2. Effect of 4-HI on immobility time in rats treated with ICH

We performed FST following the protocol schedule of 7, 14, 24, and 34 days to promote the further role of 4-HI in ALB-induced ICH in rats. On Day 01, all groups did not differ significantly. However, animals in the diseased group presented test results of depressive episodes and increasing immobility in a forced swim task. In addition, groups with autologous blood significantly increased the immobility period compared to vehicle control rats. Chronic 4-HI 100 mg/kg, the perse treatment had no activity compare to the activity reported with vehicle-treated rats. Therefore the immobility period was reduced by 4-HI 50 mg/kg and 4-HI 100 mg/kg over 35 days versus vehicle and4-HI 100 mg/kg perse treated rats [Two-way ANOVA: $F_{(15,90)} = 236.6$, $p < 0.001$] (Fig. 5).

3.2.3. Effect of 4-HI on the neurological score in rats treated with ICH

BCT was conducted on 1, 15, 25, and 35 days in assessing the potential role of 4-HI in ALB hemorrhagic rats. On day 01, no significant difference was observed between all the groups. The results have shown that ALB induced ICH rats with a more significant dysfunction in the vehicle group rats. The neurological score of 4-HI 100 mg/kg in autologous blood groups was significantly reduced compared to vehicle-treated animals. Following treatment with 4-HI 50 mg/kg and 4-HI 100 mg/kg for 35 days, neurological performance significantly improved [Two-way ANOVA: $F_{(15,90)} = 8.95$, $p < 0.001$] (Fig. 6)

3.2.4. Effect of 4-HI on locomotor activity in rats treated with ICH

Locomotor activity was also conducted on days 7, 14, 21, 28, and 35 to determine the possible impact of 4-HI in brain hemorrhagic rats. On day 01, all the groups had no significant differences. In rats, ALB induced hemorrhage comparison to vehicle-treated rats, caused a significant decrease in locomotion activity. Prolonged 4-HI 100 mg/kg Perse therapy showed no locomotive behavior improvement over vehicle-treated rats. The locomotion activity improved significantly with 4-HI 50 mg/kg and 4-HI 100 mg/kg over 35 days. [Two-way ANOVA: $F_{(20,120)} = 16.34$, $p < 0.01$] (Fig. 7).

3.2.5. Effect of 4-HI on discrimination index (DI) in rats treated with ICH

We also screened new object recognition on the 1, 15, 25, and 35 days of the protocol. We found a confirmed injury to hippocampal memory formation in rats with a decrease in memory than vehicle rats. On Day 01, all groups did not show any significance. ALB-treated groups have demonstrated a significant reduction in exploration time (DI) compared with vehicle-treated rats. The treatment in perse did not show any memory changes compared to rats in a vehicle control group. After treatment with 4-HI 50 mg/kg and 4-HI 100 mg/kg, exploration time (DI) was significantly improved [Two-way ANOVA: $F_{(15,90)} = 5.595$, $p < 0.01$] (Fig. 8).

3.3. Effect of 4-HI on cellular and molecular markers levels in ICH treated rats

3.3.1. Effect of 4-HI on IGF-1 and GLP-1 level in rats treated with ICH

4-HI mediated activation of IGF-1/GLP-1 may primarily increase the cAMP/PKA and the PI3K/Akt levels, which might also interact with IR/IGF-1R targets in CNS and mediating its neuroprotective effects. The ALB-treated group alone showed a low IGF-1/GLP-1 level compared to the vehicle control and sham control group ($p < 0.001$). The treatment of 4-HI 100 mg/kg perse did not improve as against vehicle-treated rats. The level of IGF-1/GLP-1 significantly increased during 35 days in dose-dependent post-treatment with 4-HI 50 mg/kg and 4-HI 100 mg/kg [one-way ANOVA: $F_{(5,25)} = 3.482$, $p < 0.001$], [one-way ANOVA: $F_{(5,25)} = 1.149$, $p < 0.001$] (Table 1, **column 1a and 1b).**

3.3.2. Effect of 4-HI on myelin basic protein level in rats treated with ICH

We conducted time-course testing of MBP levels using ELISA kits in brain homogenates to determine the possible effect of 4-HI in ALB-induced hemorrhagic rats. We concluded that MBP was significantly reduced in the group treated with the ALB alone than the vehicle/sham control group ($p < 0.0001$). In the vehicle control and 4-HI 100 perse group, no significant difference was found. Treatment with persistent 4-HI 100 mg/kg did not improve in comparison to vehicle-treated animals. This significantly increased the treatment dose by 4-HI 50 mg/kg at MBP levels and by 4-HI 100 mg/kg treated animals [one-way ANOVA: $F_{(5,25)} = 1.163$, $p < 0.001$] (Table 1, **column 1c).**

3.3.3. Effect of 4-HI on Bax and Bcl-2 levels in rats treated with ICH

As seen in Table 2, the Bax level in rats treated with ALB treated rats significantly increased compared to the vehicle control group, indicating that brain tissue apoptosis factors increased with illness. In contrast to the group of vehicles and sham control ($p < 0.01$), the levels of Bcl 2 in the brain tissue of rats in disease groups decreased significantly. In-vehicle control and 4-HI 100 perse group, no significant difference was found. Perse treatment showed no improvement than vehicle control rats compared to 4-HI 100 mg/kg perse treatments. The decrease in the levels of Bax
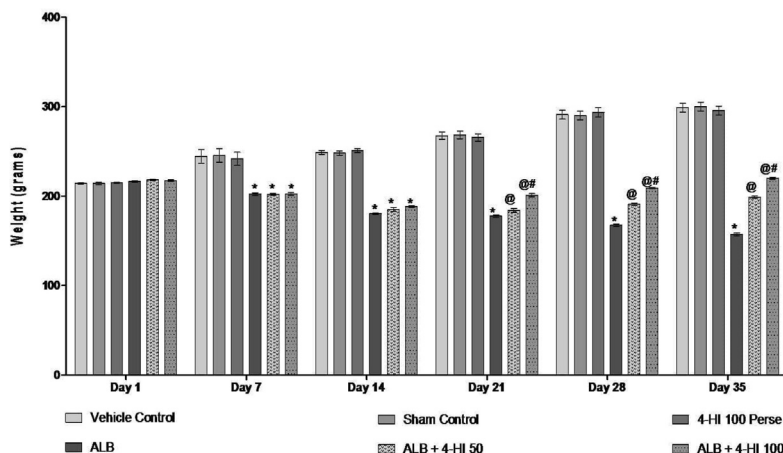
Fig. 2. Effect of 4-HI on body weight in rats treated with ICH. Two-way ANOVA was used (post-hoc Bonferroni's test), *p < 0.01 v/s vehicle control; sham control and 4-HI 100 *Per se*; @ p < 0.01 v/s ALB; @# p < 0.01 v/s ALB + 4-HI 50 (n = 6).
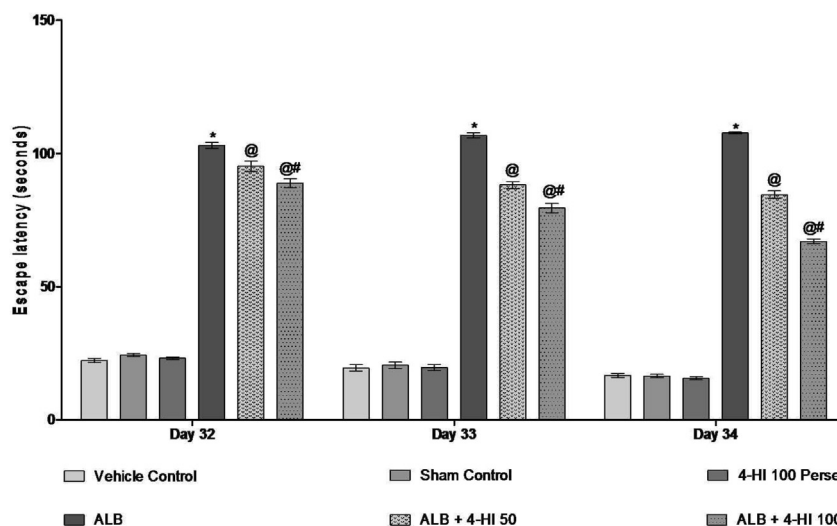
Fig. 3. Effect of 4-HI on escape latency in rats treated with ICH. Two-way ANOVA was used (post-hoc Bonferroni's test), * p < 0.01 v/s vehicle control; sham control and 4-HI 100 *Pe rse*; @ p < 0.01 v/s ALB; @# p < 0.01 v/s ALB + 4-HI 50 (n = 6).
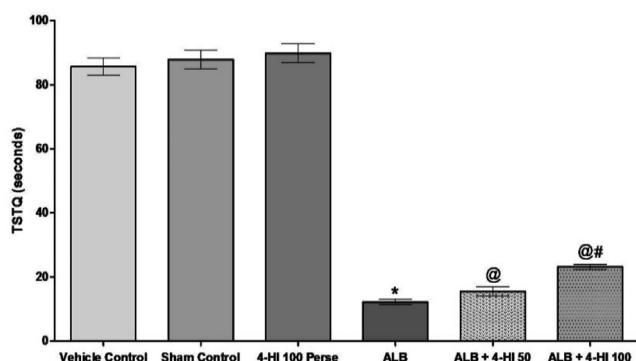
Fig. 4. Effect of 4-HI on TSTQ in rats treated with ICH. Two-way ANOVA was used (post-hoc Bonferroni's test), * p < 0.01 v/s vehicle control; sham control and 4-HI 100 *Per se*; @ p < 0.01 v/s ALB; @# p < 0.01 v/s ALB + 4-HI 50 (n = 6).

and elevated Bcl-2 levels were found significantly with 4-HI 50 mg/kg and 4-HI 100 mg/kg[one-way ANOVA: $F(5,25) = 2.213$, p < 0.01], [one-way ANOVA: $F(5,25) = 1.654$, p < 0.01] (Table 2, **Column 2a & 2b).**

3.3.4. Effect of 4-HI on Caspase-3 levels in ICH treated rats

In the process of cell apoptosis, the Caspase-3 is part of the cysteines-aspartic (caspase) families and sequential cleavages of the Caspase-3 series. These findings show that ALB in the diseased group has increased the apoptosis marker level in rats' brain tissue in the ICH model. The ALB treated group alone showed high levels of Caspase-3, in contrast to the vehicle and sham control group (p < 0.01). Also, no significant difference between the vehicle control and the 4-HI 100 perse groups was found. Continuous 4-HI 100 mg/kg perse therapy showed no decrease than rats with vehicle control. The level of Caspase-3 decreased dose-dependently and substantially in 35 days, after treatment with 4-HI 50 mg/kg and 4-HI 100 mg/kg [one-way ANOVA: $F(5,25) = 1.883$, p < 0.01] (Table 2, **Column 2c).**

3.4. Effect of 4-HI on the levels of neurotransmitters in rats treated with ICH

To investigate the potential neuroprotective effect of 4-HI in ALB-induced hemorrhagic rats, we evaluated the amounts of different neurotransmitters in brain homogenates. Only the ALB-treated group had low GABA, Ach, dopamine, and glutamate levels,
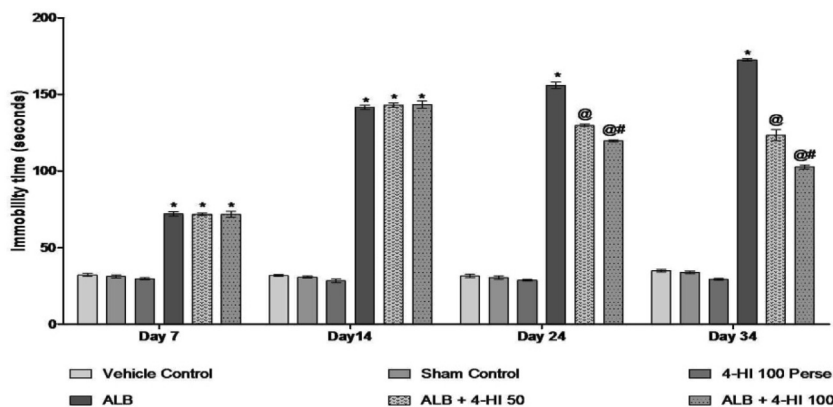
Fig. 5. Effect of 4-HI on immobility time in rats treated with ICH. Two-way ANOVA was used (post-hoc Bonferroni's test), * $p < 0.001$ v/s vehicle control; sham control and 4-HI 100 *Per se*; @ $p < 0.001$ v/s ALB; @# $p < 0.001$ v/s ALB + 4-HI 50 (n = 6).

Fig. 6. Effect of 4-HI on the neurological score in rats treated with ICH. Two-way ANOVA was used (post-hoc Bonferroni's test), * $p < 0.001$ v/s vehicle control; sham control and 4-HI 100 *Per se*; @ $p < 0.001$ v/s ALB; @# $p < 0.001$ v/s ALB + 4-HI 50 (n = 6).

Fig. 7. Effect of 4-HI on locomotor activity in rats treated with ICH. Two-way ANOVA was used (post-hoc Bonferroni's test), * $p < 0.001$ v/s vehicle control; sham control and 4-HI 100 *Per se*; @ $p < 0.001$ v/s ALB; @# $p < 0.001$ v/s ALB + 4-HI 50 (n = 6).

Fig. 8. Effect of 4-HI on discrimination index in rats treated with ICH. Two-way ANOVA was used (post-hoc Bonferroni's test), * p < 0.01 v/s vehicle control; sham control and 4-HI 100 *Per se*; @ p < 0.01 v/s ALB; @# p < 0.01 v/s ALB + 4-HI 50 (n = 6).

Table 1
Effect of 4-HI on IGF-1, GLP-1, and myelin basic protein levels in rats treated with ICH.

S. No.	Groups	Cellular and Molecular markers		
		IGF-1 (pg/mg protein) (Column 1a)	GLP-1 (pg/mg protein) (Column 1b)	Myelin Basic protein (μg/mg protein) (Column 1c)
1.	Vehicle control	73.91 ± 0.76	110.4 ± 0.45	108.7 ± 0.50
2.	Sham control	74.06 ± 0.37	112.0 ± 0.30	105.9 ± 0.30
3.	4-HI 100 *Perse*	75.01 ± 0.45	111.7 ± 0.48	106.5 ± 0.53
4.	ALB	25.67 ± 0.28*	40.86 ± 0.24*	59.24 ± 0.56*
5.	ALB + 4-HI 50	40.67 ± 0.49@	44.98 ± 0.66@	75.63 ± 0.34@
6.	ALB + 4-HI 100	56.13 ± 0.59@#	62.66 ± 0.59@#	96.78 ± 0.47@#

One-way ANOVA followed by (post-hoc Tukey's test) was used,
  * p < 0.001 v/s vehicle control; sham control and 4-HI 100 *Per se*;
  @ p < 0.001 v/s ALB;
  @# p < 0.001 v/s ALB + 4-HI 50 (n = 6).

Table 2
Effect of 4-HI on apoptotic markers in rats treated with ICH.

S. No.	Groups	Apoptotic markers		
		Bax (ng/mg protein) (Column 2a)	Bcl-2 (ng/mg protein) (Column 2b)	Caspase-3 (ng/gm) (Column 2c)
1.	Vehicle control	4.96 ± 0.38	18.30 ± 0.35	27.18 ± 0.40
2.	Sham control	5.79 ± 0.23	16.96 ± 0.33	24.42 ± 0.35
3.	4-HI 100 *Per se*	4.77 ± 0.19	18.61 ± 0.43	23.15 ± 0.71
4.	ALB	12.13 ± 0.48*	6.96 ± 0.63*	66.46 ± 0.38*
5.	ALB + 4-HI 50	8.86 ± 0.20@	12.03 ± 0.33@	54.60 ± 0.43@
6.	ALB + 4-HI 100	6.64 ± 0.19@#	15.14 ± 0.32@#	37.20 ± 0.44@#

One-way ANOVA followed by (post-hoc Tukey's test) was used,
  * p < 0.01 v/s vehicle control; sham control and 4-HI 100 *Per se*;
  @ p < 0.01 v/s ALB;
  @# p < 0.01 v/s ALB + 4-HI 50 (n = 6).

whereas the vehicle-treated and sham groups had elevated glutamate levels (p < 0.001). Treatment with *perse* showed no improvement compared to vehicle group rats for continuous treatment with 4-HI 100 mg/kg. Over 35 days in Ach, after treatment with 4-HI 50 mg/kg and 4-HI 100 mg/kg remarkably increased significantly and dose-dependently [one-way ANOVA: $F_{(5,25)} = 1.65$, p < 0.001], dopamine [one-way ANOVA: $F_{(5,25)} = 1.093$, p < 0.001], GABA[one-way ANOVA: $F_{(5,25)} = 2.051$, p < 0.001] levels and significantly decreased glutamate levels [one-way ANOVA: $F_{(5,25)} = 1.540$, p < 0.001] (Table 3).

3.5. Effect of 4-HI on inflammatory cytokines levels in rats treated with ICH

To evaluate the therapeutic effect of 4-HI in ALB-induced hemorrhagic rats, we also measured the levels of several pro-inflammatory markers in the brain, including TNF-α, IL-1β, and IL-17. The results showed that, as compared to the vehicle and 4-HI 100 mg/kg perse group. Persistent 4-HI 100 mg/kg perse treatment showed no improvement as compared to the vehicle-treated rats. However, 35 days of treatment with 4-HI 50 mg/kg and 4-HI

Table 3
Effect of 4-HI on neurotransmitters levels in ICH-treated rats.

S. No.	Groups	Neurotransmitters (ng/mg protein)			
		GABA	Glutamate	Ach	Dopamine
1.	**Vehicle control**	125.0 ± 0.42	81.10 ± 0.43	7.22 ± 0.12	97.22 ± 0.42
2.	**Sham control**	122.9 ± 0.48	80.71 ± 0.52	7.55 ± 0.17	98.18 ± 0.56
3.	**4-HI 100 *Per se***	123.5 ± 0.45	80.26 ± 0.62	7.19 ± 0.19	95.95 ± 0.67
4.	**ALB**	17.80 ± 0.74*	160.9 ± 0.65*	2.14 ± 0.14*	31.37 ± 0.46*
5	**ALB + 4-HI 50**	32.42 ± 0.37@	137.0 ± 0.79@	3.60 ± 0.22@	52.56 ± 0.57@
6.	**ALB + 4-HI 100**	53.00 ± 1.56@#	117.6 ± 0.60@#	4.88 ± 0.22@#	62.08 ± 0.45@#

One-way ANOVA followed by (post-hoc Tukey's test) was used,
* $p < 0.001$ v/s vehicle control; sham control and 4-HI 100 *Per se*;
@ $p < 0.001$ v/s ALB;
@# $p < 0.001$ v/s ALB + 4-HI 50 (n = 6).

100 mg/kg significantly and dose-dependently reduced the levels of TNF-α, IL-1β and IL-17 as compared to the ALB group [one-way ANOVA: $F_{(5,25)} = 1.066$, $p < 0.001$], [one-way ANOVA: $F_{(5,25)} = 3.618$, $p < 0.001$], [one-way ANOVA: $F_{(5,25)} = 2.587$, $p < 0.001$] (Table 4).

3.5.1. Effect of 4-HI on oxidative stress markers in rats treated with ICH

The ALB alone group showed decrease CAT, GPx, GSH and SOD levels in collation with high AchE, LDH, MDA and nitrite levels in the sham group ($p < 0.01$). Chronic treatment with 4-HI 100 mg/kg *perse* showed no better than rats with vehicle control. Oxidative stress markers have significantly decreased for 35 days of treatment with 4-HI-50 mg/kg and 4-HI-100 mg/kg compared to those with ALB only. It was noticed that the level of CAT[one-way ANOVA: $F_{(5,25)} = 1.589$, $p < 0.01$], GPx [one-way ANOVA: $F_{(5,25)} = 5.627$, $p < 0.01$], GSH[one-way ANOVA: $F_{(5,25)} = 0.8987$, $p < 0.01$], and SOD[one-way ANOVA: $F_{(5,25)} = 0.8527$, $p < 0.01$], was significantly improved and there was a low level of AchE [one-way ANOVA: $F_{(5,25)} = 1.169$, $p < 0.01$],LDH [one-way ANOVA: $F_{(5,25)} = 1.369$, $p < 0.01$], MDA [one-way ANOVA: $F_{(5,25)} = 1.716$, $p < 0.01$], and nitrite [one-way ANOVA: $F_{(5,25)} = 0.2870$, $p < 0.01$] in the brain homogenates of rats ($p < 0.01$) (Table 5a & Table 5b).

3.6. Effect of 4-HI on gross pathological alterations & hematoma size in rats treated with ICH

3.6.1. Whole brain assessment

The brain of ALB-treated rats showed visible damage and breach meninges compared to 4-HI-100 mg/kg perse, sham, and vehicle-treated groups that were optimally sized and had clearly observable meninges. 4-HI 100 mg/kg *perse* treatment for the long term showed no improvement in vehicle-treated rats. Through the administration of 4-HI, morphological improvements were significantly noticed after the administration of 4-HI 50 mg/kg and 100 mg/kg post ALB treatment (Fig. 9).

3.6.2. Brain section assessment

The clearly observed tissue of the brain was seen in the sham, vehicle, and 4-HI 100 mg/kg *perse* groups during coronal sectioning. The brains of ALB-treated group coronal areas were shown with cortical contusions, swellings, and severe subarachnoid bleeding compared to the 4-HI-perse, sham, and vehicle-treated rats. Treatment with constant 4-HI 100 mg/kg perse no improvement compared to sham and vehicle group rats has been observed. The 4-HI treatment of 50 mg/kg and 100 mg/kg reduces the autologous blood-mediated pathological alterations (Fig. 10).

3.6.3. Assessment of hematoma size

The hematoma was not significantly affected by any vehicle and sham controls, compared with 4 HI 100 mg/kg perse. In ALB-treated rats, hematoma size was considerably larger than the vehicle, sham, and the 4-HI 100 mg/kg perse groups. The treatment with prolonged 4-HI 100 mg/kg and perse rats didn't show any improvement compared with vehicle and sham control rats. Treatment with 4-HI 50 mg/kg and 4-HI 100 mg/ kg reduced hematoma significantly in comparison with groups in which autologous blood alone was used [one-way ANOVA: $F_{(5,25)} = 3.023$, $p < 0.001$] (Fig. 11).

4. Discussion

The present study demonstrated the potency of 4-HI against the ICH model induced by ALB in rats. Chronic oral administration of 4-HI at doses of 50 mg/kg and 100 mg/kg illustrated a neuroprotective effect in restoring the various ICH-related pathological foundations. ICH's consequences, the most severe phase of stroke, have not changed significantly over the years, and treatment options are generally limited to supportive care (Rajdev et al., 2020). Surgeries are usually ineffective, especially if the bleeding has entered the ventricular system. In the current study, the ICH model is used safely and effectively mimics a single ICV-autologous blood injection. It was also responsible for neurobehavioral and cognitive deficiencies that closely mimic the human hemorrhage in certain brain regions (Alharbi et al., 2016; Lu et al., 2015; Deinsberger et al., 1996; Sansing et al., 2011).

The major findings of this study were that ICV administration of ALB in the brains of rats caused ICH, 4-HI had a neuroprotective effect on restoring brain function. Furthermore, there was a definite role of IGF-1 and GLP-1 in the particular disease (Pang et al., 2017). In our study, ALB was injected into rats brains to induced ICH. Our experimental period was 35 days with very low ALB volumes (20 Âµl), resulting in insufficient blood coagulation and low mortality rates (5.2 percent) and hematoma than other studies with high blood mortality. In addition, delay/elevation of various cell and molecular markers, together with alterations in neurotransmitters, increase oxidative stress, and neuro-inflammatory markers were well reported in brain hemorrhage pathophysiology (Hou et al., 2012; Gong et al., 2001).

The body weight was significantly improved on 14, 21, and 28 days. Functional recovery decreases glutamate concentrations and increases dopamine levels, where4-HI 50 mg/kg significantly increases recognition of NOR (discrimination index) and gives a new insight into ICH treatment (Zhu et al., 2014). The forced swim test, locomotor activity, and beam crossing tasks were also significantly improved from 25 to 35 days by chronic administration of 4-HI 100 mg/kg (Gaur et al., 2012). Bleeding in these structures can lead to contusion, reducing Ach synthesis and transferring them to

Table 4
Effect of 4-HI on inflammatory cytokines levels in rats treated with ICH.

S. No.	Groups	Inflammatory markers (pg/mg protein)		
		TNF-α	IL-1β	IL-17
1.	Vehicle control	105.8 ± 0.36	78.97 ± 0.41	41.91 ± 0.31
F2.	Sham control	103.8 ± 0.33	76.99 ± 0.42	40.43 ± 0.42
3.	4-HI 100 *Per se*	104.7 ± 0.41	77.97 ± 0.41	41.06 ± 0.35
4.	ALB	309.4 ± 0.23[*]	583.4 ± 0.33[*]	650.9 ± 0.20[*]
5.	ALB + 4-HI 50	269.8 ± 0.35[@]	484.7 ± 0.41[@]	451.1 ± 0.28[@]
6.	ALB + 4-HI 100	253.2 ± 0.41[@#]	435.8 ± 0.82[@#]	251.5 ± 0.32[@#]

One-way ANOVA followed by (post-hoc Tukey's test) was used
[*] $p < 0.001$ v/s vehicle group; sham and 4-HI 100 *Per se*;
[@] $p < 0.001$ v/s ALB;
[@#] $p < 0.001$ v/s ALB + 4-HI 50 (n = 6).

Table 5a
Effect of 4-HI on oxidative stress markers levels in rats treated with ICH.

S. No.	Groups	Oxidative stress markers			
		AchE (μM/mg protein)	SOD (μM/mg protein)	GSH (μM/mg protein)	LDH (U/L)
1.	Vehicle control	13.79 ± 0.37	96.98 ± 0.47	22.34 ± 0.29	411.3 ± 0.62
2.	Sham control	13.14 ± 0.45	97.13 ± 0.54	22.29 ± 0.28	409.5 ± 0.61
3.	4-HI 100 *Per se*	13.56 ± 0.26	97.92 ± 0.46	22.66 ± 0.45	410.4 ± 0.59
4.	ALB	50.36 ± 0.44[*]	30.54 ± 1.73[*]	6.17 ± 0.20[*]	1018 ± 36.29[*]
5.	ALB + 4-HI 50	32.85 ± 0.47[#]	59.73 ± 0.57[#]	8.91 ± 0.19[#]	805.2 ± 13.23[#]
6.	ALB + 4-HI 100	25.15 ± 0.43#@	70.86 ± 0.33#@	12.04 ± 0.19#@	657.1 ± 11.22#@

One-way ANOVA followed by (post-hoc Tukey's test) was used. [*]$p < 0.01$ v/s vehicle control; sham control and 4-HI 100 *Per se*; [@]$p < 0.01$ v/s ALB; [@#]$p < 0.01$ v/s ALB + 4-HI 50; (n = 6).

Table 5b
Effect of 4-HI on oxidative stress markers levels in ALB induced brain hemorrhagic rats.

S. No.	Groups	Oxidative stress markers			
		GPx (ng/mg protein)	MDA (nM/mg protein)	Nitrite (μM/mg protein)	Catalase (nmol/min/mg protein)
1.	Vehicle control	20.97 ± 0.20	3.18 ± 0.30	4.21 ± 0.37	18.74 ± 0.12
2.	Sham control	19.05 ± 0.19	3.61 ± 0.35	4.56 ± 0.30	18.75 ± 0.09
3.	4-HI 100 *Per se*	20.19 ± 0.19	3.37 ± 0.23	4.47 ± 0.25	18.65 ± 0.11
4.	ALB	7.30 ± 0.26[*]	16.17 ± 0.35[*]	14.15 ± 0.49[*]	5.67 ± 0.08[*]
5.	ALB + 4-HI 50	10.61 ± 0.49[@]	8.41 ± 0.22[@]	8.77 ± 0.19[@]	9.56 ± 0.07[@]
6.	ALB + 4-HI 100	12.79 ± 0.50[@#]	5.04 ± 0.17[@#]	6.04 ± 0.08[@#]	12.03 ± 0.13[@#]

One-way ANOVA followed by (post-hoc Tukey's test) was used.
[*] $p < 0.01$ v/s vehicle control; sham control and 4-HI 100 *Per se*;
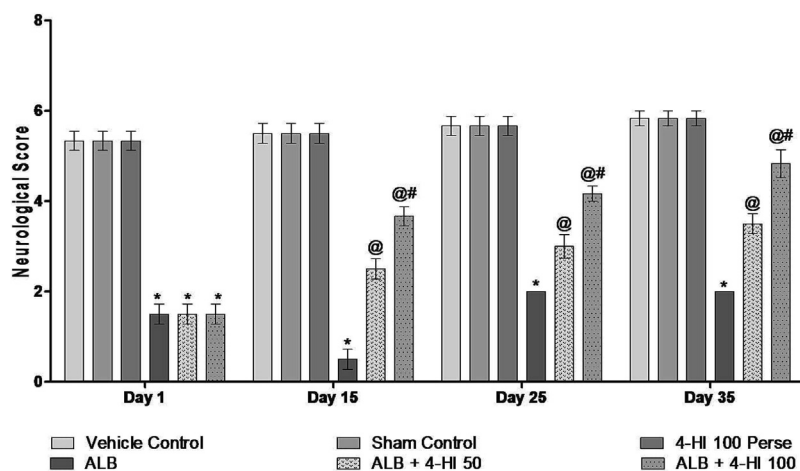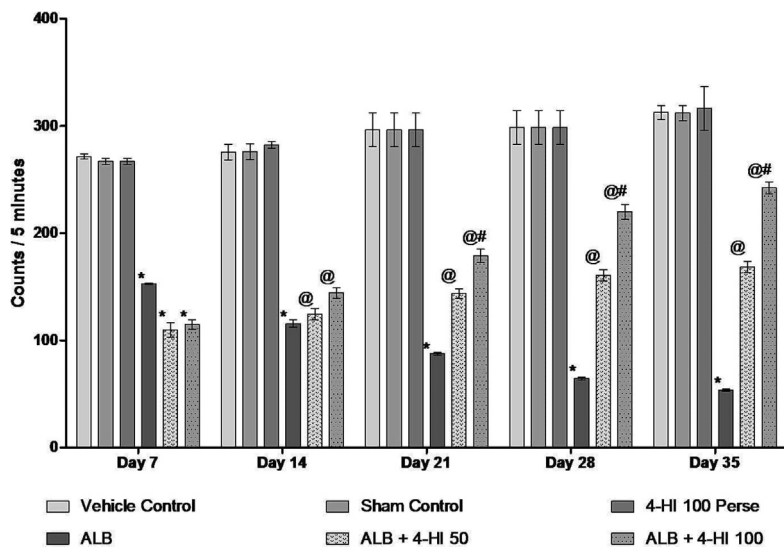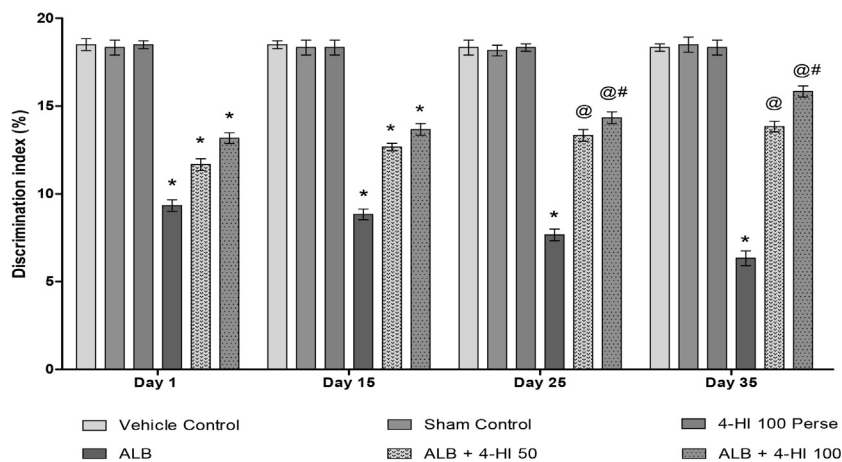[@] $p < 0.001$ v/s ALB;
[@#] $p < 0.001$ v/s ALB + 4-HI 50 (n = 6).

other brain areas affecting learning and memory(Zhang and Plotkin, 2004; Myhrer, 2003).

In the present study, 4-HI 100 mg/kg decreases the escape latency and increases the TSTQ during spatial navigation tasks in MWM (Kodumuri et al., 2019). It also reduced high AchE levels and raised the Ach levels, resulting in cognitive changes by increasing the basal forebrain cholinergic system. 4-HI also helped improve GABA levels and reduced oxidative stress confirming the beneficial impact of 4-HI 50 mg/kg and 100 mg/kg on main molecular ICH mechanisms. These findings indicate that ALB-mediated ICH causes oxidative stress, elevated inflammatory cytokines, and altered neurotransmitter levels, reinforcing neuropathological alterations in the rat brain with prolonged 4-HI administration.

The development of hematoma has led to cognitive impairment, increased Caspase-3 (Cao et al., 2018) and BAX (Bai et al., 2019), level while decreased MBP (Khan et al., 2006) and Bcl-2 (Keshavarz et al., 2013) levels in ALB-treated rats. Moreover, alleviate the elevated oxidative stress AchE (Ellman et al., 1961), LDH (Mehan et al., 2017), MDA (Mehan et al., 2020), nitrite concentration (Singh et al., 2017), and decreased CAT, GSH (Alam et al.,

2020), GPx (Fathimoghadam et al., 2019), SOD (Cai et al., 2015) concentration, elevated level of inflammatory cytokines (TNF-α, IL-1β, IL-17) (Wang et al., 2018), decreased neurotransmitters Ach (Zeng et al., 2017), DOPA (Jamwal and Kumar, 2016), GABA, glutamate (Rajdev et al., 2020) in the hemorrhagic brain.

The current study has limitations because we could do immune histochemistry following the Western blot, but it would surely lead to a very long study. But in conclusion, we tried to give our best input to the study with the required efforts and dedication to making the study stronger, more interesting, and efficient.

Despite its promising neuroprotective (Broca et al., 2000), anti-diabetic (Broca et al., 2004), anti-dyslipidemic, and anti-oxidant activity, the exact mechanism of action of 4-HI has still not been appropriately understood (Yadav et al.,2011). For a consecutive 35 days, the 4-HI administration significantly improves motor and behavioral dysfunction, oxidative damage, neuroinflammation, showing its many target activities in complexes in particular molecular and cellular ways. Caspase-3 and Bax-2 activation associated with cell death and inflammation of neurons caused by cerebral hemorrhages (Cao et al., 2018). Long-term therapy with 4-HI
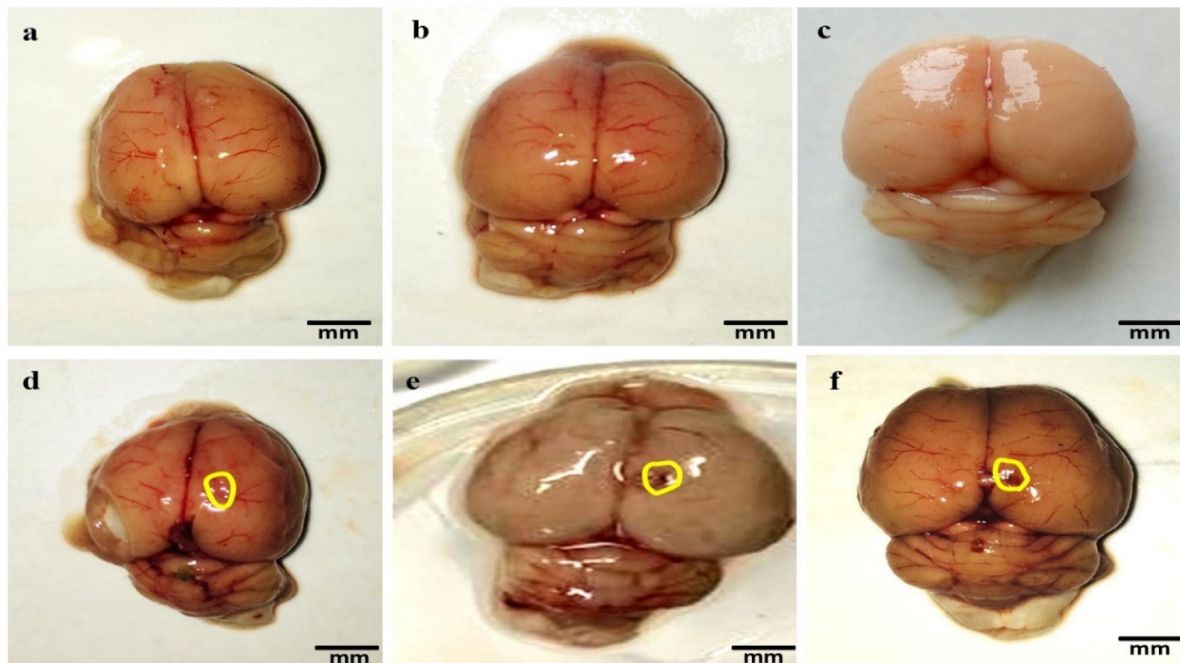
Fig. 9. Neuroprotective effect of 4-HI on gross pathological changes (whole rat brain) in ALB induced brain hemorrhagic rats (a) Vehicle control (b) Sham control(c) 4-HI 100 *Perse* (d) ALB (e) ALB + 4-HI 50 (f) ALB + 4-HI 100 (Scale bar = 5 mm). **Note:** Yellow circles are pointing to the site of the brain injury.
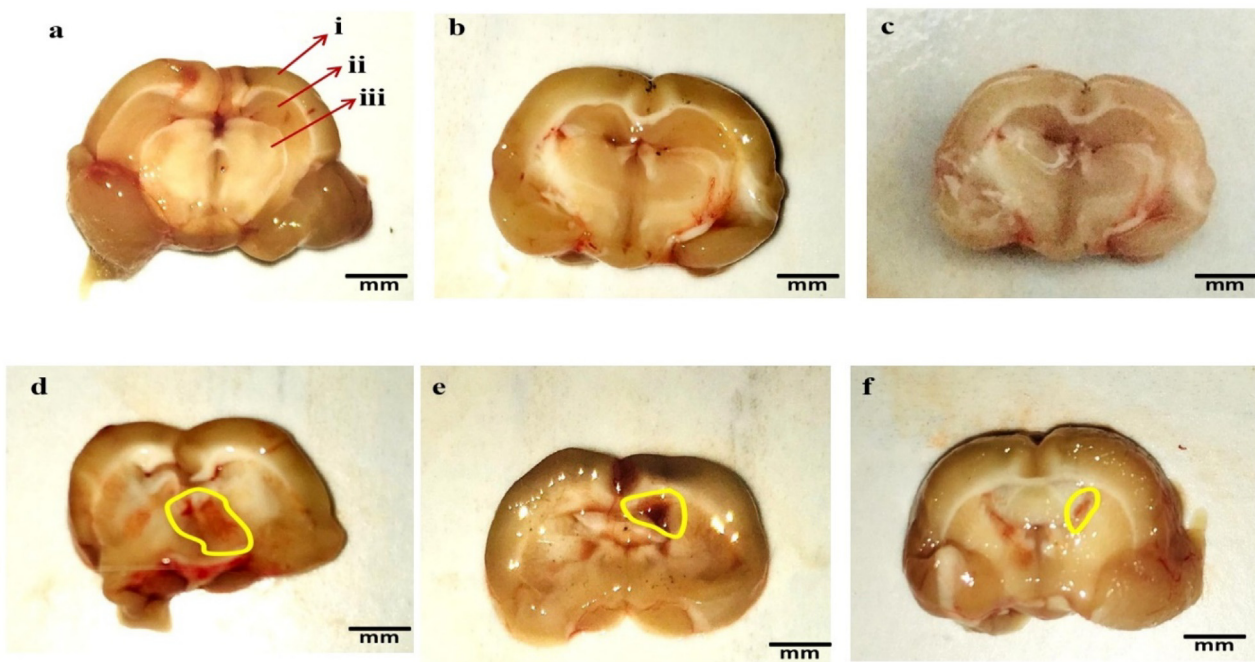
Fig. 10. Neuroprotective effect of 4-HI on gross pathological changes (brain sections) in ALB induced brain hemorrhagic rats (a) Vehicle control i. Cerebral cortex ii. Hippocampus iii. Basal ganglia (b) Sham control(c) 4-HI 100 *Perse* (d) ALB (e) ALB + 4-HI 50 (f) ALB + 4-HI 100 (Scale bar = 5 mm). **Note:** Yellow circles are pointing to the site of the brain injury.

50 mg/kg and 4-HI 100 mg kg had raised the neurological score in specific behavioral parameters, reflecting its significant neuroprotective role in patients in reducing inflammation and neuronal mortality.

In addition, it also improved the IGF-1/GLP-1 level in the brain, along with the improvement of Bax, Bcl-2, and Caspase-3 (Athauda and Foltynie, 2016). The level of MBP was also significantly improved with the administration of 4-HI chronically. In this study, gross pathological alterations and expressions of various biomarkers, followed by the neurological dysfunctions after hemorrhage in the rats' brain, were examined. The findings showed the neuroprotective effect of 4-HI, suggesting that this animal model is satisfactorily provable and manageable. The hematoma volume was also evaluated and gave us an improved and adequate response to our protocol drug.
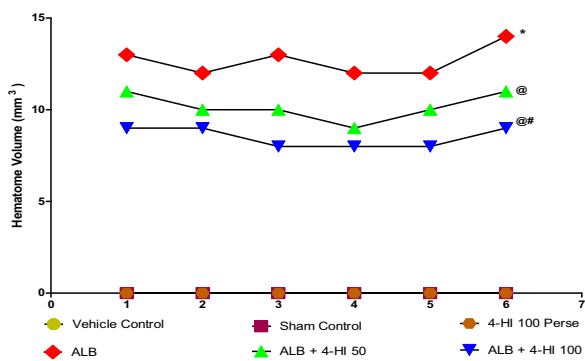
Fig. 11. Effect of 4-HI on hematoma size in rats treated with ICH. One-way ANOVA followed by (post-hoc Tukey's test) was used. * p < 0.001 v/s vehicle control; sham control and 4-HI 100 *Per se*; @ p < 0.001 v/s ALB; @# p < 0.001 v/s ALB + 4-HI 50 (n = 6).

However, the overall findings of the current study indicate the neuroprotective activity of 4-HI in ALB-induced neurobehavioral, neurochemical, and morphological changes in brain hemorrhagic-treated rats by activating IGF-1/GLP-1 mediated signaling pathways. However, the current findings are primarily correlations in which the neuroprotective function of 4-HI in ALB-induced neurobehavioral and neurochemical changes in ICH-treated rats was mainly studied via activating IGF-1 and GLP-1 mediated signalling pathways and MBP restoration. A further mechanism of action, such as IGF-1/GLP-1 signalling pathway overexpression or deletion, must be validated, and additional molecular confirmation, such as immunoblotting and immunohistopathology, will be required in the future.

5. Conclusions

In continuation, ICH animals experienced acute memory and cognitive losses; motor weakness caused by cellular and molecular dysfunction, neurochemical disturbance, elevated oxidative stress and elevated neuroinflammatory markers. Here, we focused on improving the sign and symptoms related to ICH and thus providing symptomatic relief. Chronic 4-HI 50 mg/kg and 100 mg/kg therapy tend to provide a possible neuroprotective effect by improving behavioral and neurochemical deficits. A significant elevation was noticed in the IGF-1/GLP-1 levels in the brain, which promptly says that 4-HI must have been acted on the IGF-1R/GLP-1R, insulin, and tyrosine kinase receptors. Furthermore, the MBP and apoptotic markers' levels were also noticed to be slightly improved, accompanied by improved hematoma size. The level of different neurotransmitters, oxidative stress, and neuroinflammatory markers in the brain has been found to have improved with the administration of 4-HI therapy. 4-HI may also present a potential drug approach with post-cerebral hemorrhagic and neurobehavioral alterations to ameliorate neurological impairments.

6. Data availability statement

No new data were created or analyzed in this study. Data sharing is not applicable to this article. All data generated or analyzed during this study are included in this article. There are no separate or additional files.

Funding

CRediT authorship contribution statement

Declaration of Competing Interest

The authors declare that they have no known competing financial interests or personal relationships that could have appeared to influence the work reported in this paper.

Acknowledgments

References

Abdel-Rahman, R.F., Alqasoumi, S.I., Ogaly, H.A., Abd-Elsalam, R.M., El-Banna, H.A., Soliman, G.A., 2020. Propolis ameliorates cerebral injury in focal cerebral ischemia/reperfusion (I/R) rat model via upregulation of TGF-β1. Saudi Pharmaceutical Journal 28 (1), 116–126. https://doi.org/10.1016/j.jsps.2019.11.013.

Aebi, H. 1984. Catalase in vitro. In: Methods in enzymology, vol. 105, pp. 121-126, Academic Press. https://doi.org/10.1016/S0076-6879(84)05016-3

Alam, M., Minj, E., Yadav, R., Mehan, S., 2020. Neuroprotective Potential of Adenyl Cyclase/cAMP/CREB and Mitochondrial CoQ10 Activator in Amyotrophic Lateral Sclerosis Rats. Curr. Bioact. Compd. 16, 1. https://doi.org/10.2174/1573407216999200723113054.

Alharbi, B.M., Tso, M.K. and Macdonald, R.L., 2016. Animal models of spontaneous intracerebral hemorrhage. Neurological research, 38(5), pp.448-455. https://doi.org/10.1080/01616412.2016.1144671.

Aronowski, J., Hall, C.E., 2005. New horizons for primary intracerebral hemorrhage treatment: experience from preclinical studies. Neurol. Res. 27 (3), 268–279. https://doi.org/10.1179/016164105X25225.

Athauda, D., Foltynie, T., 2016. The glucagon-like peptide 1 (GLP) receptor as a therapeutic target in Parkinson's disease: mechanisms of action. Drug Discovery Today 21 (5), 802–818. https://doi.org/10.1016/j.drudis.2016. 01.013.

Avalos-Soriano, A., De la Cruz-Cordero, R., Rosado, J.L., Garcia-Gasca, T., 2016. 4-Hydroxyisoleucine from Fenugreek (Trigonella foenum-graecum): Effects on Insulin Resistance Associated with Obesity. Molecules (Basel, Switzerland) 21 (11), 1596. https://doi.org/10.3390/molecules21111596.

Baggio, L.L., Drucker, D.J., 2014. Glucagon-like peptide-1 receptors in the brain: controlling food intake and body weight. J. Clin. Investigation 124 (10), 4223–4226. https://doi.org/10.1172/JCI78371.

Baquer, N.Z., Kumar, P., Taha, A., Kale, R.K., Cowsik, S.M., McLean, P., 2011. Metabolic and molecular action of Trigonella foenum-graecum (fenugreek) and trace metals in experimental diabetic tissues. Journal of biosciences, 36(2), pp.383-396. https://doi.org/10.1007/s12038-011-9042-0.

Bai, M., Liu, B., Peng, M., Jia, J., Fang, X., Miao, M., 2019. Effect of Sargentodoxa cuneata total phenolic acids on focal cerebral ischemia reperfusion injury rats model. Saudi journal of biological sciences, 26(3), pp.569-576. https://doi.org/10.1016/j.sjbs.2018.11.019.

Bertilsson, G., Patrone, C., Zachrisson, O., Andersson, A., Dannaeus, K., Heidrich, J., Wikström, J., 2008. Peptide hormone exendin-4 stimulates subventricular zone neurogenesis in the adult rodent brain and induces recovery in an animal model of Parkinson's disease. J. Neurosci. Res. 86 (2), 326–338. https://doi.org/10.1002/jnr.21483.

Boyko, M., Azab, A.N., Kuts, R., Gruenbaum, B.F., Gruenbaum, S.E., Melamed, I., Brotfain, E., Shapira, Y., Cesnulis, E. and Zlotnik, A., 2013. The neuro-behavioral profile in rats after subarachnoid hemorrhage. Brain research, 1491, pp.109-116. https://doi.org/10.1016/j.brainres.2012.10.061.

Broca, C., Breil, V., Cruciani-Guglielmacci, C., Manteghetti, M., Rouault, C., Derouet, M., Ktorza, A., 2004. Insulinotropic agent ID-1101 (4-hydroxyisoleucine) activates insulin signaling in rat. Am. J. Physiol.-Endocrinol. Metab. 287 (3), E463–E471. https://doi.org/10.1152/ajpendo.00163.2003.

Broca, C., Manteghetti, M., Gross, R., Baissac, Y., Jacob, M., Petit, P., Ribes, G., 2000. 4-Hydroxyisoleucine: effects of synthetic and natural analogues on insulin secretion. Eur. J. Pharmacol. 390 (3), 339–345.

Cabou, C., Burcelin, R., 2011. GLP-1, the gut-brain, and brain-periphery axes. Rev. Diabetic Stud.: RDS 8 (3), 418. https://doi.org/10.1900/RDS.2011.8.418.

Cai, J., Cao, S., Chen, J., Yan, F., Chen, G., Dai, Y., 2015. Progesterone alleviates acute brain injury via reducing apoptosis and oxidative stress in a rat experimental subarachnoid hemorrhage model. Neurosci. Lett. 600, 238–243.

Candeias, E., Sebastiao, I., Cardoso, S., Carvalho, C., Santos, M.S., Oliveira, C.R., Duarte, A.I., 2018. Brain GLP-1/IGF-1 signaling and autophagy mediate exendin-4 protection against apoptosis in type 2 diabetic rats. Mol. Neurobiol. 55 (5), 4030–4050. https://doi.org/10.1007/s12035-017-0622-3.

Cao, L., Miao, M., Qiao, J., Bai, M., Li, R., 2018. The protective role of verbenalin in rat model of focal cerebral ischemia reperfusion. Saudi J. Biol. Sci.25 (6), 1170–1177. https://doi.org/10.1016/j.sjbs.2017.10.005.

Carro, E., Trejo, J.L., Núñez, A., Torres-Aleman, I., 2003. Brain repair and neuroprotection by serum insulin-like growth factor I. Mol. Neurobiol. 27 (2), 153–162. https://doi.org/10.1385/mn:27:2:153.

Cohen, S.J., Stackman Jr, R.W., 2015. Assessing rodent hippocampal involvement in the novel object recognition task. A review. Behav. Brain Res. 285, 105–117. https://doi.org/10.1016/j.bbr.2014.08.002.

D'Ambrosio, A.L., Sughrue, M.E., Yorgason, J.G., Mocco, J.D., Kreiter, K.T., Mayer, S.A., Connolly Jr, E.S., 2005. Decompressive hemicraniectomy for poor-grade aneurysmal subarachnoid hemorrhage patients with associated intracerebral hemorrhage: clinical outcome and quality of life assessment. Neurosurgery 56 (1), 12–20. https://doi.org/10.1227/01.NEU.0000144820.38439.63.

Deinsberger, W., Vogel, J., Kuschinsky, W., Michael Auer, L., Böker, D.K., 1996. Experimental intracerebral hemorrhage: description of a double injection model in rats. Neurol. Res. 18 (5), 475–477. https://doi.org/10.1080/01616412.1996.11740456.

Donzanti, B.A., Yamamoto, B.K., 1988. An improved and rapid HPLC-EC method for the isocratic separation of amino acid neurotransmitters from brain tissue and microdialysisperfusates. Life Sci. 43 (11), 913–922. https://doi.org/10.1016/0024-3205(88)90267-6.

Dudi, R., Mehan, S., 2018. Neuroprotection of brain permeable Forskolin ameliorates behavioral, biochemical and histopathological alterations in rat model of intracerebral hemorrhage. Pharmaspire 10 (2).

Duggal, P., Mehmood Siddiqui, E., Singh Jadaun, K., Mehan, S., 2020. Investigation of Low Dose Cabazitaxel Potential as Microtubule Stabilizer in Experimental Model of Alzheimer's Disease: Restoring Neuronal Cytoskeleton. Curr. Alzheimer Res. 17, 1–15.

Ellman, G.L., 1959. Tissue sulfhydryl groups. Arch. Biochem. Biophys. 82 (1), 70–77.

Ellman, G.L., Courtney, K.D., Andres Jr, V., Featherstone, R.M., 1961. A new and rapid colorimetric determination of acetylcholinesterase activity. Biochem. Pharmacol. 7 (2), 88–95. https://doi.org/10.1016/0006-2952(61)90145-9.

Fathimoghadam, H., Farbod, Y., Ghadiri, A., Fatemi, R., 2019. Moderating effects of crocin on some stress oxidative markers in rat brain following demyelination with ethidium bromide. Heliyon 5, (2). https://doi.org/10.1016/j.heliyon.2019.e01213 e01213.

Gao, F., Jian, L., Zafar, M.I., Du, W., Cai, Q., Shafqat, R.A., Lu, F., 2015. 4-Hydroxyisoleucine improves insulin resistance in HepG2 cells by decreasing TNF-α and regulating the expression of insulin signal transduction proteins. Mol. Med. Rep. 12 (5), 6555–6560. https://doi.org/10.3892/mmr.2015.4298.

Gaur, V., Bodhankar, S.L., Mohan, V., Thakurdesai, P., 2012. Antidepressant-like effect of 4-hydroxyisoleucine from Trigonellafoenum graecum L. seeds in mFice. Biomed. Aging Pathol. 2 (3), 121–125. https://doi.org/10.1016/j.biomag.2012.07.002.

Geloneze, B., de Lima-Júnior, J.C., Velloso, L.A., 2017. Glucagon-like peptide-1 receptor agonists (GLP-1RAs) in the brain–adipocyte axis. Drugs 77 (5), 493–503. https://doi.org/10.1007/s40265-017-0706-4.

Gengler, S., McClean, P.L., McCurtin, R., Gault, V.A., Hölscher, C., 2012. Val (8) GLP-1 rescues synaptic plasticity and reduces dense core plaques in APP/PS1 mice. Neurobiol. Aging 33 (2), 265–276. https://doi.org/10.1016/j.neurobiolaging.2010.02.014.

Gong, C., Boulis, N., Qian, J., Turner, D.E., Hoff, J.T., Keep, R.F., 2001. Intracerebral hemorrhage-induced neuronal death. Neurosurgery 48 (4), 875–883. https://doi.org/10.1097/00006123-200104000-00037.

Grieco, M., Giorgi, A., Gentile, M.C., d'Erme, M., Morano, S., Maras, B., Filardi, T., 2019. Glucagon-like peptide-1: a focus on neurodegenerative diseases. Front. Neurosci. 13, 1112. https://doi.org/10.3389/fnins.2019.01112.

Harkavyi, A., Whitton, P.S., 2010. Glucagon-like peptide 1 receptor stimulation as a means of neuroprotection. Br. J. Pharmacol. 159 (3), 495–501. https://doi.org/10.1111/j.1476-5381.2009.00486.x.

Heppner, F.L., Ransohoff, R.M., Becker, B., 2015a. Immune attack: the role of inflammation in Alzheimer disease. Nat. Rev. Neurosci. 16 (6), 358–372. https://doi.org/10.1038/nrn3880.

Heppner, K.M., Kirigiti, M., Secher, A., Paulsen, S.J., Buckingham, R., Pyke, C., Grove, K.L., 2015b. Expression and distribution of glucagon-like peptide-1 receptor mRNA, protein and binding in the male nonhuman primate (Macaca mulatta) brain. Endocrinology 156 (1), 255–267. https://doi.org/10.1210/en.2014-1675.

Himeno, T., Kamiya, H., Naruse, K., Harada, N., Ozaki, N., Seino, Y., Fukami, A., 2011. Beneficial effects of exendin-4 on experimental polyneuropathy in diabetic mice. Diabetes 60 (9), 2397–2406. https://doi.org/10.2337/db10-1462.

Holt, M.K., Trapp, S., 2016. The physiological role of the brain GLP-1 system in stress. Cogent Biol. 2 (1), 1229086. https://doi.org/10.1080/23312025.2016.1229086.

Hou, J., Manaenko, A., Hakon, J., Hansen-Schwartz, J., Tang, J., Zhang, J.H., 2012. Liraglutide, a long-acting GLP-1 mimetic, and its metabolite attenuate inflammation after intracerebral hemorrhage. J. Cerebral Blood Flow Metab., 32(12), 2201-2210. , https://doi.org/10.1016/S0014-2999(00)00030-3

Jamwal, S., Kumar, P., 2016. Spermidine ameliorates 3-nitropropionic acid (3-NP)-induced striatal toxicity: possible role of oxidative stress, neuroinflammation, and neurotransmitters. Physiol. Behav. 155, 180–187. https://doi.org/10.1016/j.physbeh.2015.12.015.

Javanshir, R., Hemmati, M., 2020. The effect of coenzyme Q10 supplementation on oxidative stress status and insulin resistance in diabetic rats. J. Birjand Univ. Med. Sci. 27 (2), 139–149.

Katsurada, K., Yada, T., 2016. Neural effects of gut-and brain-derived glucagon-like peptide-1 and its receptor agonist. J. Diabetes Investigation 7, 64–69. https://doi.org/10.1111/jdi.12464.

Keshavarz, M., Emamghoreishi, M., Nekooeian, A.A., Warsh, J.J., Zare, H.R., 2013. Increased bcl-2 protein levels in rat primary astrocyte culture following chronic lithium treatment. Iranian journal of medical sciences, 38(3), p.255.

Khan, O.H., Enno, T.L., Del Bigio, M.R., 2006. Brain damage in neonatal rats following kaolin induction of hydrocephalus. Experimental neurology, 200(2), pp.311-320. https://doi.org/10.1016/j.expneurol.2006.02.113.

Kirkman, M.A., Allan, S.M., Parry-Jones, A.R., 2011. Experimental intracerebral hemorrhage: avoiding pitfalls in translational research. J. Cereb. Blood Flow Metab. 31 (11), 2135–2151. https://doi.org/10.1038/jcbfm.2011.124.

Kodumuri, P.K., Thomas, C., Jetti, R., Pandey, A.K., 2019. Fenugreek seed extract ameliorates cognitive deficits in streptozotocin-induced diabetic rats. J. Basic Clin. Physiol. Pharmacol. 30 (4).

Kumar, N., Sharma, N., Khera, R., Gupta, R., Mehan, S., 2021. Guggulsterone ameliorates ethidium bromide-induced experimental model of multiple sclerosis via restoration of behavioral, molecular, neurochemical and morphological alterations in rat brain. Metab. Brain Dis. https://doi.org/10.1007/s11011-021-00691-x.

Kumar, P., Kale, R.K., McLean, P., Baquer, N.Z., 2012. Antidiabetic and neuroprotective effects of Trigonellafoenum-graecum seed powder in diabetic rat brain. Prague Med. Rep. 113 (1), 33–43.

Labandeira-Garcia, J.L., Costa-Besada, M.A., Labandeira, C.M., Villar-Cheda, B., Rodríguez-Perez, A.I., 2017. Insulin-like growth factor-1 and neuroinflammation. Front. Aging Neurosci. 9, 365. https://doi.org/10.3389/fnagi.2017.00365.

Lee, Y.S., Jun, H.S., 2016. Anti-inflammatory effects of GLP-1-based therapies beyond glucose control. Mediators Inflammation 2016. https://doi.org/10.1155/2016/3094642.

Liu, M., Zhang, C., Liu, W., Luo, P., Zhang, L., Wang, Y., Fei, Z., 2015. A novel rat model of blast-induced traumatic brain injury simulating different damage degree: implications for morphological, neurological, and biomarker changes. Front. Cellular Neurosci. 9, 168. https://doi.org/10.3389/fncel.2015.00168.

Llewellyn-Smith, I.J., Reimann, F., Gribble, F.M., Trapp, S., 2011. Preproglucagon neurons project widely to autonomic control areas in the mouse brain. Neuroscience 180, 111–121. https://doi.org/10.1016/j.neuroscience.2011.02.023.

Lu, W., Wen, J., 2020. Neuroprotective roles of total flavones of Camellia on early brain injury andcognitive dysfunction following subarachnoid hemorrhage in rats. Metabolic Brain Disease, pp.1-9. https://doi.org/10.1007/s11011-020-00567-6.

Mehan, S., Monga, V., Rani, M., Dudi, R., Ghimire, K., 2018. Neuroprotective effect of solanesol against 3-nitropropionic acid-induced Huntington's disease-like behavioral, biochemical, and cellular alterations: Restoration of coenzyme-Q10-mediated mitochondrial dysfunction. Indian J. Pharmacol. 50 (6), 309. https://doi.org/10.4103/ijp.IJP_11_18.

Mehan, S., Parveen, S., Kalra, S., 2017. Adenyl cyclase activator forskolin protects against Huntington's disease-like neurodegenerative disorders. Neural Regenerat. Res. 12 (2), 290. https://doi.org/10.4103/1673-5374.200812.

Mehan, S., Rahi, S., Tiwari, A., Kapoor, T., Rajdev, K., Sharma, R., Dudi, R., 2020. Adenylate cyclase activator forskolin alleviates intracerebroventricular propionic acid-induced mitochondrial dysfunction of autistic rats. Neural Regenerat. Res. 15 (6), 1140. https://doi.org/10.4103/1673-5374.270316.

Minj, E., Upadhayay, S., Mehan, S., 2021. Nrf2/HO-1 Signaling Activator Acetyl-11-keto-beta Boswellic Acid (AKBA)-Mediated Neuroprotection in Methyl Mercury-Induced Experimental Model of ALS. Neurochem. Res. https://doi.org/10.1007/s11064-021-03366-2.

Moghadam, F.H., Vakili-Zarch, B., Shafiee, M., Mirjalili, A., 2013. Fenugreek seed extract treats peripheral neuropathy in pyridoxine induced neuropathic mice. EXCLI J. 12, 282.

Mohammed, A., Islam, M., 2018. Spice-derived bioactive ingredients: potential agents or food adjuvant in the management of diabetes mellitus. Front. Pharmacol. 9, 893.

Moneim, A.E.A., 2015. The neuroprotective effect of berberine in mercury-induced neurotoxicity in rats. Metabolic Brain Dis. 30 (4), 935–942. https://doi.org/10.1007/s11011-015-9652-6.

Myhrer, T., 2003. Neurotransmitter systems involved in learning and memory in the rat: a meta-analysis based on studies of four behavioral tasks. Brain Res. Rev. 41 (2–3), 268–287. https://doi.org/10.1016/S0165-0173(02)00268-0.

Nadeau, C.A., Dietrich, K., Wilkinson, C.M., Crawford, A.M., George, G.N., Nichol, H.K., Colbourne, F., 2019. Prolonged Blood-Brain Barrier Injury Occurs After Experimental Intracerebral Hemorrhage and Is Not Acutely Associated with

Additional Bleeding. Translational Stroke Res. 10 (3), 287–297. https://doi.org/10.1007/s12975-018-0636-9.

Nadjar, A., Berton, O., Guo, S., Leneuve, P., Dovero, S., Diguet, E., Tison, F., Zhao, B., Holzenberger, M. and Bezard, E., 2009. IGF-1 signaling reduces neuro-inflammatory response and sensitivity of neurons to MPTP. Neurobiology of aging, 30(12), pp.2021-2030. https://doi.org/ 10.1016/j.neurobiolaging.2008.02.009

Nieto-Estévez, V., Defterali, Ç., Vicario-Abejón, C., 2016. IGF-I: a key growth factor that regulates neurogenesis and synaptogenesis from embryonic to adult stages of the brain. Front. Neurosci. 10, 52. https://doi.org/10.3389/fnins.2016.00052.

Nieuwkamp, D.J., de Gans, K., Rinkel, G.J., Algra, A., 2000. Treatment and outcome of severe intraventricular extension in patients with subarachnoid or intracerebral hemorrhage: a systematic review of the literature. J. Neurol. 247 (2), 117–121. https://doi.org/10.1007/PL00007792.

Nuttall, F.Q., Schweim, K.J., Gannon, M.C., 2006. Effect of orally administered phenylalanine with and without glucose on insulin, glucagon and glucose concentrations. Horm. Metab. Res. 38 (08), 518–523.

Ola, M.S., Aleisa, A.M., Al-Rejaie, S.S., Abuohashish, H.M., Parmar, M.Y., Alhomida, A. S., Ahmed, M.M., 2014. Flavonoid, morin inhibits oxidative stress, inflammation and enhances neurotrophic support in the brain of streptozotocin-induced diabetic rats. Neurol. Sci. 35 (7), 1003–1008. https://doi.org/10.1007/s10072-014-1628-5.

Pang, Y., Zheng, B., Campbell, L.R., Fan, L.W., Cai, Z., Rhodes, P.G., 2010. IGF-1 can either protect against or increase LPS-induced damage in the developing rat brain. Pediatr. Res. 67 (6), 579–584. https://doi.org/10.1203/PDR.0b013e3181dc240f.

Pang, Y., Zheng, B., Campbell, L.R., Fan, L.W., Cai, Z. and Rhodes, P.G., 2010. IGF-1 can either protect against or increase LPS-induced damage in the developing rat brain. Pediatric research, 67(6), pp.579-584. https://doi.org/10.1203/PDR.0b013e3181dc240f.

Park, S.E., Dantzer, R., Kelley, K.W., McCusker, R.H., 2011. Central administration of insulin-like growth factor-I decreases depressive-like behavior and brain cytokine expression in mice. J. Neuroinflammat. 8 (1), 1–14. https://doi.org/10.1186/1742-2094-8-12.

Porcari, G.S., Beslow, L.A., Ichord, R.N., Licht, D.J., Kleinman, J.T., Jordan, L.C., 2018. Neurologic Outcome Predictors in Pediatric Intracerebral Hemorrhage: A Prospective Study. Stroke 49 (7), 1755–1758. https://doi.org/10.1161/STROKEAHA.118.021845.

Power, C., Henry, S., Del Bigio, M.R., Larsen, P.H., Corbett, D., Imai, Y., Peeling, J., 2003. Intracerebral hemorrhage induces macrophage activation and matrix metalloproteinases. Ann. Neurol. 53 (6), 731–742. https://doi.org/10.1002/ana.10553.

Powers, W.J., 2010. Intracerebral hemorrhage and head trauma: common effects and common mechanisms of injury. Stroke 41 (10 Suppl), S107–S110. https://doi.org/10.1161/STROKEAHA.110.595058.

Rahi, S., Gupta, R., Sharma, A., Mehan, S., 2021. Smo-Shh signaling activator purmorphamine ameliorates neurobehavioral, molecular, and morphological alterations in an intracerebroventricular propionic acid-induced experimental model of autism. Hum. Exp. Toxicol. https://doi.org/10.1177/09603271211013456.

Rajdev, K., Mehan, S., 2019. Neuroprotective Methodologies of Co-Enzyme Q10 Mediated Brain Hemorrhagic Treatment: Clinical and Pre-Clinical Findings. CNS& Neurological Disorders-Drug Targets (Formerly Current Drug Targets-CNS & Neurological Disorders),18(6) 446-465. https://doi.org/10.2174/1871527318666190610101144

Rajdev, K., Siddiqui, E.M., Jadaun, K.S., Mehan, S., 2020. Neuroprotective potential of solanesol in acombined model of intracerebral and intraventricular hemorrhage in rats. IBRO Rep. https://doi.org/10.1016/j.ibror.2020.03.001.

Rampogu, S., Parameswaran, S., Lemuel, M.R., Lee, K.W., 2018. Exploring the Therapeutic Ability of Fenugreek against Type 2 Diabetes and Breast Cancer Employing Molecular Docking and Molecular Dynamics Simulations. Evidence-based Complementary Alternative Med. : eCAM 2018, 1943203. https://doi.org/10.1155/2018/1943203.

Ren, P., Wang, B.C., Wang, Y.Z., Hao, S.L., Guo, T.W., Li, X.F., 2018. Evaluating tensile damage of brain tissue in intracerebral hemorrhage based on strain energy. Exp. Therap. Med. 16 (6), 4843–4852. https://doi.org/10.3892/etm.2018.6757.

Rodriguez-Perez, A.I., Borrajo, A., Diaz-Ruiz, C., Garrido-Gil, P., Labandeira-Garcia, J. L., 2016. Crosstalk between insulin-like growth factor-1 and angiotensin-II in dopaminergic neurons and glial cells: role in neuroinflammation and aging. Oncotarget 7 (21), 30049. https://doi.org/10.18632/oncotarget.9174.

Roh, J.H., Ko, I.G., Kim, S.E., Lee, J.M., Ji, E.S., Kim, J.H., Chang, H.K., Lee, S.K., Kim, K.H., 2016. Treadmill exercise ameliorates intracerebral hemorrhage-induced depression in rats. Journal of exercise rehabilitation, 12(4), p.299. https://doi.org/10.12965/jer.1632692.346.

Rossi, S., Furlan, R., De Chiara, V., Motta, C., Studer, V., Mori, F., Battistini, L., 2012. Interleukin-1β causes synaptic hyperexcitability in multiple sclerosis. Ann. Neurol. 71 (1), 76–83. https://doi.org/10.1002/ana.22512.

Rowlands, J., Heng, J., Newsholme, P., Carlessi, R., 2018. Pleiotropic effects of GLP-1 and analogs on cell signaling, metabolism, and function. Front. Endocrinol. 9, 672. https://doi.org/10.3389/fendo.2018.00672.

Sansing, L.H., Kasner, S.E., McCullough, L., Agarwal, P., Welsh, F.A., Kariko, K., 2011. Autologous blood injection to model spontaneous intracerebral hemorrhage in mice. JoVE (J. Visualized Exp.) 54. https://doi.org/10.3791/2618.

Santi, A., Genis, L., Torres Aleman, I., 2018. A coordinated action of blood-borne and brain insulin-like growth factor I in the response to traumatic brain injury. Cerebral Cortex 28 (6), 2007–2014. https://doi.org/10.1093/cercor/bhx106.

Serhan, A., Aerts, J.L., Boddeke, E.W., Kooijman, R., 2020. Neuroprotection by Insulin-like Growth Factor-1 in Rats with Ischemic Stroke is Associated with Microglial Changes and a Reduction in Neuroinflammation. Neuroscience 426, 101–114. https://doi.org/10.1016/j.neuroscience.2019.11.035.

Sevrin, T., Boquien, C.Y., Gandon, A., Grit, I., de Coppet, P., Darmaun, D., Alexandre-Gouabau, M.C., 2020. Fenugreek Stimulates the Expression of Genes Involved in Milk Synthesis and Milk Flow through Modulation of Insulin/GH/IGF-1 Axis and Oxytocin Secretion. Genes 11 (10), 1208.

Shandilya, A., Mehan, S., 2021. Dysregulation of IGF-1/GLP-1 signaling in the progression of ALS: potential target activators and influences on neurological dysfunctions. Neurol. Sci.: Off. J. Italian Neurological Soc. Italian Soc. Clin. Neurophysiol. https://doi.org/10.1007/s10072-021-05328-6.

Sharma, N., Upadhayay, S., Shandilya, A., Sahu, R., Singh, A., Rajkhowa, B., Mehan, S., 2021. Neuroprotection by solanesol against ethidium bromide-induced multiple sclerosis-like neurobehavioral, molecular, and neurochemical alterations in experimental rats. Phytomedicine Plus 1 (4). https://doi.org/10.1016/j.phyplu.2021.100051.

Sharma, R., Rahi, S., Mehan, S., 2019. Neuroprotective potential of solanesol in intracerebroventricular propionic acid induced experimental model of autism: Insights from behavioral and biochemical evidence. Toxicol. Rep. 6, 1164–1175. https://doi.org/10.1016/j.toxrep.2019.10.019.

Shiraishi, D., Fujiwara, Y., Komohara, Y., Mizuta, H., Takeya, M., 2012. Glucagon-like peptide-1 (GLP-1) induces M2 polarization of human macrophages via STAT3 activation. Biochem. Biophys. Res. Commun. 425 (2), 304–308. https://doi.org/10.1016/j.bbrc.2012.07.086.

Singh, N., Bansal, Y., Bhandari, R., Marwaha, L., Singh, R., Chopra, K., Kuhad, A., 2017. Naringin reverses neurobehavioral and biochemical alterations in intracerebroventricular collagenase-induced intracerebral hemorrhage in rats. Pharmacology, 100(3-4), pp.172-187. https://doi.org/10.1159/000453580.

Suh, H.S., Zhao, M.L., Derico, L., Choi, N., Lee, S.C., 2013. Insulin-like growth factor 1 and 2 (IGF1, IGF2) expression in human microglia: differential regulation by inflammatory mediators. J. Neuroinflammat. 10 (1), 805. https://doi.org/10.1186/1742-2094-10-37.

Terai, K., Suzuki, M., Sasamata, M., Miyata, K., 2003. Amount of bleeding and hematoma size in the collagenase-induced intracerebral hemorrhage rat model. Neurochem. Res. 28 (5), 779–785. https://doi.org/10.1023/A:1022826220469.

Tien, L.T., Lee, Y.J., Pang, Y., Lu, S., Lee, J.W., Tseng, C.H., Fan, L.W., 2017. Neuroprotective effects of intranasal IGF-1 against neonatal lipopolysaccharide-induced neurobehavioral deficits and neuronal inflammation in the substantia nigra and locus coeruleus of juvenile rats. Dev. Neurosci. 39 (6), 443–459. https://doi.org/10.1159/000477898.

Tiwari, A., Khera, R., Rahi, S., Mehan, S., Makeen, H.A., Khormi, Y.H., Rehman, M.U., Khan, A., 2021. Neuroprotective Effect of α-Mangostin in Ameliorating Propionic Acid-Induced Experimental Model of Autism in Wistar Rats. Brain Sci. 2021 (11), 288. https://doi.org/10.3390/brainsci11030288.

Tschoe, C., Bushnell, C.D., Duncan, P.W., Alexander-Miller, M.A., Wolfe, S.Q., 2020. Neuroinflammation after intracerebral hemorrhage and potential therapeutic targets. J. Stroke 22 (1), 29. https://doi.org/10.5853/jos.2019.02236.

Uozumi, Y., Sakowitz, O., Orakcioglu, B., Santos, E., Kentar, M., Haux, D., Unterberg, A., 2014. Decompressive craniectomy in patients with aneurysmal subarachnoid hemorrhage: a single-center matched-pair analysis. Cerebrovas. Dis. (Basel, Switzerland) 37 (2), 109–115. https://doi.org/10.1159/000356979.

Wang, J., Tsirka, S.E., 2005. Tuftsin fragment 1–3 is beneficial when delivered after the induction of intracerebral hemorrhage. Stroke 36 (3), 613–618. https://doi.org/10.1161/01.STR.0000155729.12931.8f.

Wang, J., Hu, Z., Yang, S., Liu, C., Yang, H., Wang, D., Guo, F., 2018. Inflammatory cytokines and cells are potential markers for patients with cerebral apoplexy in intensive care unit. Exp. Therap. Med. 16 (2), 1014–1020. https://doi.org/10.3892/etm.2018.6213.

Wang, X.W., Yuan, L.J., Yang, Y., Zhang, M., Chen, W.F., 2020. IGF-1 inhibits MPTP/MPP+-induced autophagy on dopaminergic neurons through the IGF-1R/PI3K-Akt-mTOR pathway and GPER. Am. J. Physiol.-Endocrinol. Metab. 319 (4), E734–E743. https://doi.org/10.1016/j.neuroscience.2019.11.035.

Wang, X., Mori, T., Sumii, T., Lo, E.H., 2002. Hemoglobin-induced cytotoxicity in rat cerebral cortical neurons: caspase activation and oxidative stress. Stroke 33 (7), 1882–1888. https://doi.org/10.1161/01.STR.0000020121.41527.5D.

Wrigley, S., Arafa, D., Tropea, D., 2017. Insulin-like growth factor 1: at the crossroads of brain development and aging. Front. Cellular Neurosci. 11, 14. https://doi.org/10.3389/fncel.2017.00014.

Xue, M., Del Bigio, M.R., 2003. Comparison of brain cell death and inflammatory reaction in three models of intracerebral hemorrhage in adult rats. J. Stroke Cerebrovasc. Dis. 12 (3), 152–159. https://doi.org/10.1016/S1052-3057(03)00036-3.

Xue, M., Del Bigio, M.R., 2000. Intracerebral injection of autologous whole blood in rats: time course of inflammation and cell death. Neuroscience letters, 283(3), pp.230-232. https://doi.org/10.1016/S0304-3940(00)00971-X.

Yadav, R., Kaushik, R., Gupta, D., 2011. The health benefits of Trigonellafoenum-graecum: A review. Int. J. Eng. Res. Appl. 1 (1), 32–35.

Zeng, Q.H., Jiang, Y.L., Wang, Y., Nie, H.X., Zhou, F., Yu, S.H., Zhang, H.J., 2017. The correlation between noradrenaline and acetylcholine levels and autonomic nervous system dysfunction in patients with stroke-associated pneumonia. Int. J. Clin. Exp. Med. 10 (10), 14761–14769.

Zhang, H., Plotkin, R.C., Wang, G., Sandel, M.E., Lee, S., 2004. Cholinergic augmentation with donepezil enhances recovery in short-term memory and sustained attention after traumatic brain injury. Arch. Phys. Med. Rehabilitat. 85 (7), 1050–1055. https://doi.org/10.1016/j.apmr.2003.10.014.

Zhou, C., Chen, R., Gao, F., Zhang, J., Lu, F., 2020. 4-Hydroxyisoleucine relieves inflammation through iRhom2-dependent pathway in co-cultured macrophages and adipocytes with LPS stimulation. BMC Complementary Med. Therap. 20 (1), 373. https://doi.org/10.1186/s12906-020-03166-1.

Zhu, W., Gao, Y., Chang, C.F., Wan, J.R., Zhu, S.S., Wang, J., 2014. Mouse models of intracerebral hemorrhage in ventricle, cortex, and hippocampus by injections of autologous blood or collagenase. PLoS ONE 9, (5). https://doi.org/10.1371/journal.pone.0097423 e97423.